C H A P T E R O N E

INTRODUCTION

1.1 BACKGROUND

Due to the critical condition of industrial fuels which include oil, gas and others, the development of renewable energy sources is continuously improving. This is the reason why renewable energy sources have become more important these days. Few other reasons include advantages like abundant availability in nature, eco-friendly and recyclable. Many renewable energy sources like solar, wind, hydel and tidal are there. Among these renewable sources solar and wind energy are the world's fastest growing energy resources. With no emission of pollutants, energy conversion is done through wind and PV cells.

Day by day, the demand for electricity is rapidly increasing. But the available base load plants are not able to supply electricity as per demand. So these energy sources can be used to bridge the gap between supply and demand during peak loads. This kind of small scale stand-alone power generating systems can also be used in remote areas where conventional power generation is impractical .

In this thesis, a wind-photovoltaic hybrid power generation system model is studied and simulated. A hybrid system is more advantageous as individual power generation system is not completely reliable. When any one of the system is shutdown the other can supply power. A block diagram of entire hybrid system is shown in figure (1.1) below.

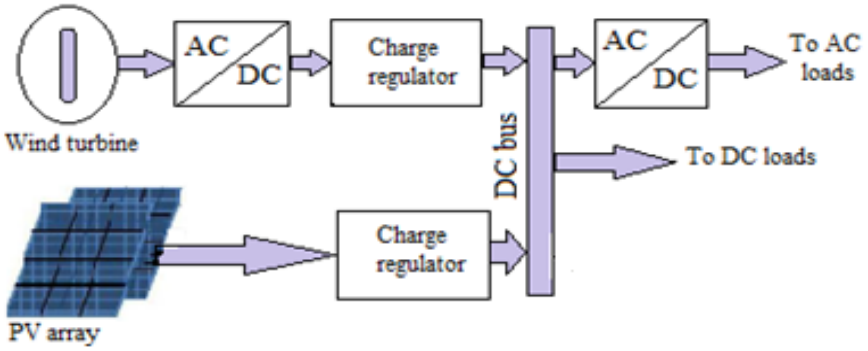

Fig(1.1). Block Diagram Of Hybrid System

The entire hybrid system comprises of PV and the wind systems. The PV system is powered by the solar energy which is abundantly available in nature. PV modules, maximum power point tracing systems make the PV energy system. The light incident on the PV cells is converted into electrical energy by solar energy harvesting means. Which extracts the maximum possible power from the PV modules the ac-dc converter is used.

Wind turbine, gear box, generator and an AC– DC converter are included in Wind turbine, gear box, generator and an AC – DC converter are included in the wind energy system. The wind turbine is used to convert wind energy to rotational mechanical energy and this mechanical energy available at the turbine shaft is converted to electrical energy using a generator.

1.2 LITERATURE REVIEW

Since both wind turbines and photovoltaics use renewable energy resources to generate electricity, the benefit of combining them into a single system can be significant. The combined system of photovoltaics and wind turbines is usually referred to as a hybrid system. In addition, a battery system, diesel engine or micro hydro systems can also operate in parallel with this hybrid system to meet load requirements [1]. Researchers face a very challenging task to increase the total energy production from the system at the lowest cost and reliability [2-5]. Wind turbines are used to convert wind energy into mechanical energy and then into electrical energy. Whatever the electrical energy generated by this system is alternative and unstable. So some controllers or inverters are used to make it continuous and store in the battery. This energy is used for household or other purposes. A group of photovoltaic cells that contain solar panels in series or in parallel, convert solar energy into electrical energy.

This energy is in the form of DC and controller power for AC or DC loads. This system has high daily electricity generation capacity, low manufacturing cost, low maintenance and has other advantages as well [3,4]. By using this kit in the hybrid system, they have succeeded in improving the power output of the system. The power generated from this system is used for street lighting and other devices. Any combination of solar and wind energy. The hybrid system can get enough power from both sources, and even if the power from one source is low at this point, it will be compensated for by the other source. Hybrid systems have gained popularity in the past, for applications in remote systems such as radio communications and satellite earth stations, or in locations not accessible by conventional power grids [6,7].

Hence, a hybrid power system is defined as a combination of two or more types of power generation systems, which is the combination of a solar energy system with a wind turbine system to form a hybrid renewable energy system. Since the power production from this

renewable energy is ultimately dependent on climatic conditions such as temperature, solar radiation, wind speed, etc. The two generation sources are individually controlled, their output going to the DC bus line to feed the isolated DC load or To the inverter section of the system to download AC power [8,9]. Thus, it can be deduced that the hybrid system that combines solar and wind generation units with storage means can decrease the fluctuation of these sources and reduce the storage capacity. Aphotovoltaic hybrid system, which uses PV energy combined with another energy source such as wind energy or diesel, is cheaper and more efficient than a photovoltaic system alone [10] .

1.3 HYBRID SYSTEM (PV&WIND) REQUIREMENTS

It is very important to develop the hybrid system (PV&WIND) and to investigate its effectiveness, we must scrutinize the tests and for four seasons of the year and investegations for modelling and evidencing difficulties as much as possible, taking into account the following data.

1.3.1 Attention And Observance of Meteorological Data

Site meteorological analysis should be done for best performance. It is important to take full advantage of the solar / wind energy sources. As choosing the right place is the desired result. All data must be measured by the hour, by day, within a year, according to weather or climate change, such as wind strength, solar radiation, and temperature [11].

1.3.2 Load Demand

It is necessary part of system to design & analyse. To find out the exact load demand it is very complicated and difficult to decide. Load variation for different seasons is not predictable, so system has to be designed for nearer or more than load demand to full fill requirements [11].

1.3.3 System Configuration

By studying all data like solar radiation, wind speed and load demand proper selection of equipment have to be made. But sizing of system will be according to the environmental conditions. Because producing power from solar-wind is depend upon the location which is to be selected [11].

1.4 THESISS MOTIVATION

In this thesis a proposed PV and wind models is used to estimate the energy output of PV / wind system installed in Libya. The results show that with hybrid system energy saving could be

achieved. As Libya relies on the oil and gas for electricity generation, these will reduce the country revenue when the load demands increase in near future. Furthermore the adoption of the PV and wind systems in Libya could help in creating awareness between people for the rational use of electricity in addition to reducing the CO2 emission.

1.5 OBJECTIVE OF THE THESISS

The objective of this thesis is to model grid-connected PV/Wind hybrid power system (MGs) at steady state and study, their transient responses to changing inputs. From this model, the output power from the two energy resources will be determined. The input for this model is solar radiation and wind speed. In this case, Libyan weather data will be used in order to investigate the potential of the hybrid PV/Wind system. The main objective could be summarized in the following points:-

- To study and model PV cell, PV array and PV panels.
- To study the characteristic curves and effect of variation of environmental conditions like irradiation and temperature.
- To trace the maximum power point of operation the PV panel irrespective of the changes in the environmental conditions.
- To study and simulate the wind power system and track its maximum power point.
- To study the behaviours of the system during steady state and sudden changes in wind speed and irradiance.

1.6 THESISS OUTLINE

The thesis has been organized into five chapters. Following the chapter one introduction, the rest of the thesis is outlined as follows .

Chapter 2 represents the modelling of wind turbine system in detail and the influence of solar radiation and temperature. The explanation was also done using illustrations and algebraic equations.

Chapter 3 explains detailed modelling of the photoelectric (PV) array with explanations of maximum power point tracking, control systems as well as illustrations and algebraic equations.

Chapter 4 presents the overall configuration of the hybrid microgrid system and all the simulation results, using MATLAB/ SIMULINK .

Chapter 5 provides comprehensive summary and conclusions of the work undertaken in this thesis and also acknowledge about the future work. The references taken for the purpose of research work are also the part of this chapter.

C H A P T E R TWO

WIND POWER SYSTEM

2.1 INTRODUCTION

Three phase AC power systems have existed for over 100 years due to their efficient transformation of ac power at different voltage levels and over long distance as well as the inherent characteristic from fossil energy driven rotating machines. Recently more renewable power conversion systems are connected in low voltage ac distribution systems as distributed generators or ac micro grids due to environmental issues caused by conventional fossil fuelled power plants [4] .

Wind energy (wind flow causes the turbine blades to convert from mechanical energy to electrical energy), and is a source of renewable energy that comes from the flow of air across the Earth's surface. This wind turbine collects kinetic energy and converts it into usable energy that can supply electricity to homes, fields, schools, or work on a small or large scale.

Wind energy is one of the fastest new sources of electricity generation in the world today, and the most important advantages of this energy are the following.

a. Green Energy: Electricity produced from wind energy is "clean" because its generation does not produce any pollution or waste gases.
b. Sustainable: Wind is a renewable energy resource that is inexhaustible and does not require fuel along to energy production.
c. Affordable: Wind energy is a source of electricity at competitive prices, due in large part to technological advances, the lack of maintenance and spare parts, and a large shelf life.
d. Economic development: Wind energy is the electricity produced locally.

2.2 WIND TURBINES

It is well known that wind is a form of solar energy. Wind is caused by the uneven heating of the atmosphere by sunlight, irregularities in the earth's surface, and the rotation of the earth. Wind flow patterns are modified according to terrain, water bodies, and vegetation. Wind flow, or kinetic energy, can be used by modern wind turbines to generate electricity .

With the use of power of the wind, wind turbines produce electricity to drive an electrical generator. Usually wind passes over the blades, generating lift and exerting a turning force inside the nacelle the rotating blades turn a shaft then goes into a gearbox, the gearbox helps in increasing the rotational speed for the operation of the generator and utilizes magnetic fields to convert the rotational energy into electrical energy. The basic components of a wind turbine system are shown in figure below figure (2.1).

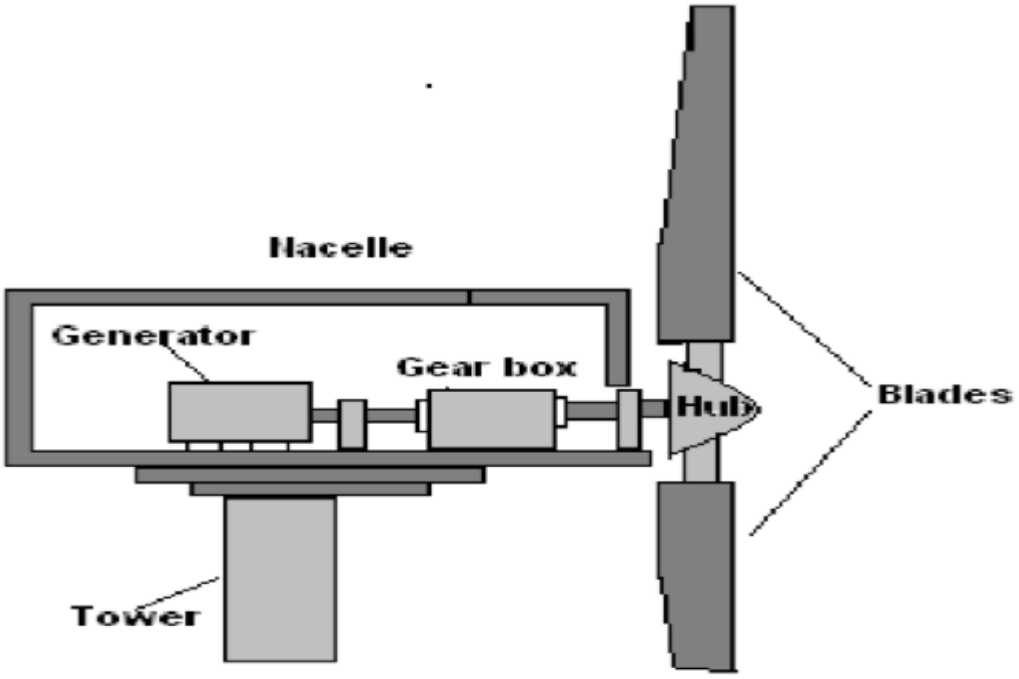

Fig (2.1). Major Turbine Components

Then the output electrical power goes to a transformer, which converts the electricity to the appropriate voltage for the power collection system. A wind turbine extracts kinetic energy from the swept area of the blades .The power contained in the wind is given by the kinetic energy of the flowing air mass per unit time [12]. Wind turbines can be distinguished into 2 categories, fixed speed and variable speed wind turbines.

The fixed speed wind turbines are connected directly to the utility grid and operate with the synchronous speed of the grid angular frequency regardless of the wind speed. The fluctuations in the wind generate mechanical stresses to the generator. Furthermore, since the wind generation system is connected to the utility grid directly, the fluctuations of the wind appear on the electrical side. The variable speed wind turbines operate in an opposite way. The speed of the generator is varied according to the wind speed solving the problem of the mechanical stresses. As a result, the output voltages of the generator have variable amplitudes and frequencies. Hence there must be a grid interconnection to convert the variable magnitude and frequency voltages of the wind turbines to the synchronous frequency of the supply grid [13-15].

2.3 TYPES OF WIND TURBINES

Wind turbines have two different types of micro-electricity generation, which means that they can be easily installed in the home and others to generate electricity. Both types of wind turbines have advantages and disadvantages.

2.3.1 A Horizontal Axis Wind Turbines (HAWT)

Horizontal axis wind turbines (HAWT) when speaking of giant wind turbines that stand along coastal lines or across vast fields. Due to their high efficiency and large power output, they are the most widely used turbines especially in commercial and industrial operation sites [16-18]

2.3.1.1 The Horizontal Axis Wind Turbine Consists Of The Following

The components can be identified from the following figure (2.2) [17].

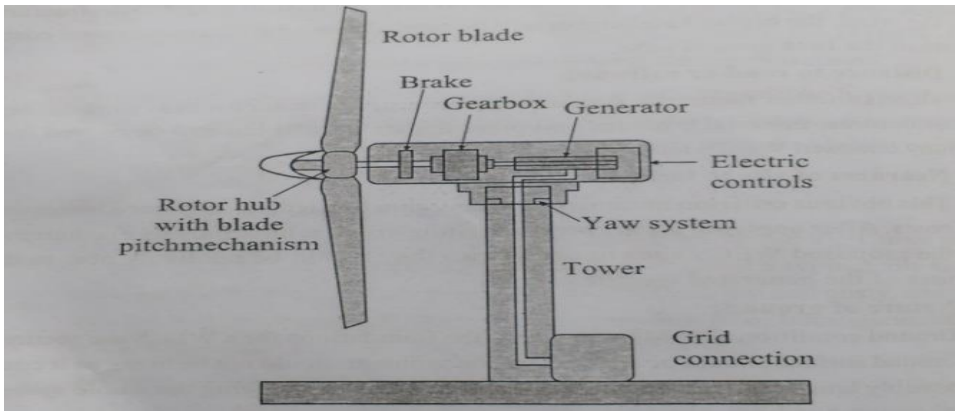

Fig (2.2). (HAWT)

a) Rotor And Blades

The rotor of a horizontal axis wind turbine (HAWT) has three long blades attached to the tower or horizontal shaft. , The rotor blades are aerodynamically shaped so that they can capture thrust from wind. Then the lifting force generates torque and thus the blades are rotated and consequently the turbine rotates.

A typical modern horizontal axis wind turbine (HAWT) has a length of 40 to 90 meters

b) Nacil

Connected to the rotor, the nacelle contains the operational components that are connected to the wind turbine generator. Its components are gearbox, alternator, brakes and control unit.

c) Yaw System

Located at the top of the tower and connected to the nickname, the diffraction system aligns the turbine towards the wind. This ensures that the wind turbine always faces the oncoming wind, which is essential for the rotor blades to catch the wind and initiate the spin.

d) Designed For Large Scale Wind Power Generation

Horizontal axis wind turbines are capable of greater power output and higher energy efficiency ideal for large scale wind power plants and electricity generation. For this reason, they dominate the wind energy industry as a major renewable energy solution [16].

2.3.1.2 Advantages Of HAWT

Variable blade pitches provides the suitable angle of attack and greater control along with good efficiency. It is located on taller towers therefore subjected to some greater wind speeds. Usually a 10m increase in the height of a tower provide 20% increment in wind speed. Since the blade moves at an angle complementary to that of the wind speed therefore drag forces are greatly reduced which causes increment in the power output [17].

2.3.1.3 Disadvantages Of HAWT :

Greater construction costs for the larger structures. Also the transportation cost increases significantly. Production of noises affect the radar operations. Great wind speed and turbulences may lead to that of structural failure. Additional Yaw Controlled mechanisms are required [19].

2.3.2 a Vertical Axis Wind Turbines (VAWT)

Vertical axis wind turbines are less affected by frequent changes in wind direction with the horizontal axis rotating the blades on the rotor shaft perpendicular to the ground. With the blades and shaft installed this way, the turbine does not need to rotate to follow the direction of the wind. The shaft was installed close to a site and the reason was that the column and its components were installed on the tower as in the following figure 2.5. On locations such as rooftops or buildings in which electricity is to be generated [16]

2.3.2.1 Types of Vertical Axis Wind Turbine

There are primarily two types of VAWT; Darrius and Savonius wind turbine.

a) Darrieus Wind Turbine.

This type was invented in 1931 by Georges Darrieus. It works with at least two blades that are vertically oriented and revolve around a vertical shaft. These turbines are high speed and low torque machine that generate AC electricity.

The generator of the turbine is located at the bottom of its blades. Blades are mounted with the help of a monopole. There are few guy wires connected to the pole that keeps the pole in place when the wind flow rotates the blades as in the figure (2.3).

One of the main drawbacks of this kind of turbine is, it cannot start by its own. So, an external power source is required to make it rotate as the initial torque is quite low.

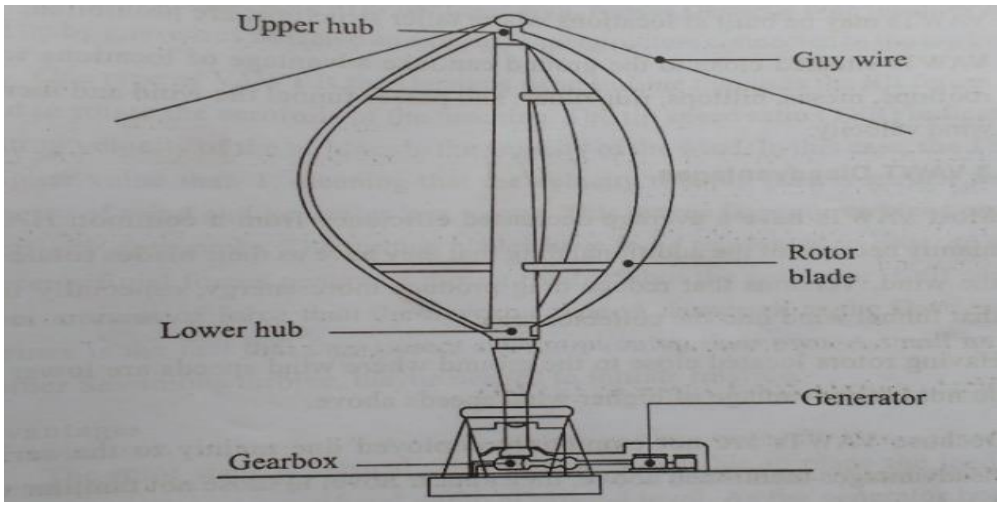

Fig (2.3). Darrieus Wind Turbines

Some Of The Main Features Of The Darrieus Wind Turbines Are:

1- These turbines are great in terms of efficiency compared to the Savonius turbines.

2- It requires an outside source of power to start.

3- Turbines with more blade are more efficient.

4- High efficiency, low reliability.

b) Savonius Wind Turbines

Savonius wind turbines on the other hand, are low speed and high torque machine. Instead of using blades, this one uses scoops to capture wind energy. Each turbine has two or more scoops to produce electricity. The scoops turn around when the wind energy applies positive force on the front side of the scoops and a negative force on the back of the scoops.

Instead of using lift generated air foil shaped blades, savonius wind turbines use drag, and that's the reason why they don't rotate the scoops faster than the wind speed as in the figure (2.4).

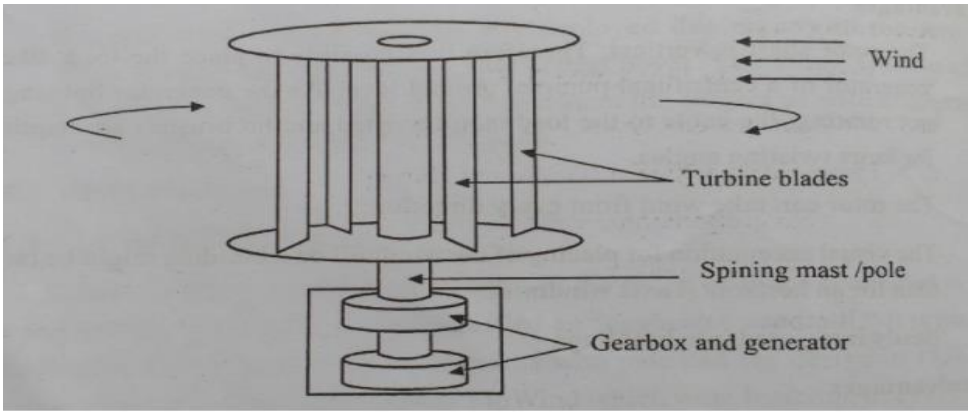

Fig (2.4). Savonius Wind Turbines

2.3.2.2 A dvantages of VAWT

Mounted close to the ground so tall structures are not required. It is having less cost and easier maintenance, lower start up speed and very lower noise. Yaw control mechanisms are not required.

2.3.2.3 Disadvantages of VAWT

It has lower efficiency due to that of the additional drag forces, due to lower height they can't capture great wind speed at the higher altitudes, and generally they need some additional start up mechanism as they are having zero starting torque.

2.4 WIND TURBINE OPERATION

The primary cause of atmospheric air motion, or wind, is uneven heating of Earth by solar radiation. For example, land and water along a coastline absorb radiation differently, and this creates the light winds or breezes normally found along a coast. Earth's rotation is also an important factor in creating winds.

Available power in the wind passing through a given area at any given velocity is due to the kinetic energy of the wind speed and is given by [19-22].

1) 0~4.5 m/s , Wind speed is too low for generating power. Turbine is not operational. Rotor is locked .
2) 4.5~11 m/s , 4.5m/s is the minimum operational speed. It is called "Cut-in speed". In 4.5 ~ 11m/s wind, generated power increases with the wind speed .
3) 11~22 m/s , Typical wind turbines reach the rated power (maximum operating power) at wind speed of 11m/s (called Rated wind speed). Further increase in wind speed will not result in substantially higher generated power by design. This is accomplished by, for example, pitching the blade angle to reduce the turbine efficiency.
4) 22 < m/s , Turbine is shut down when wind speed is higher than 22m/s (called "Cut-out" speed) to prevent structure failure.

2.5 WIND SPEED

Wind speed largely determines the amount of electricity generated by a turbine. Higher wind speeds generate more power because stronger winds allow the blades to rotate faster. [21] Faster rotation translates to more mechanical power and more electrical power from the generator. The relationship between wind speed and power for a typical wind turbine is shown in Figure (2.5).

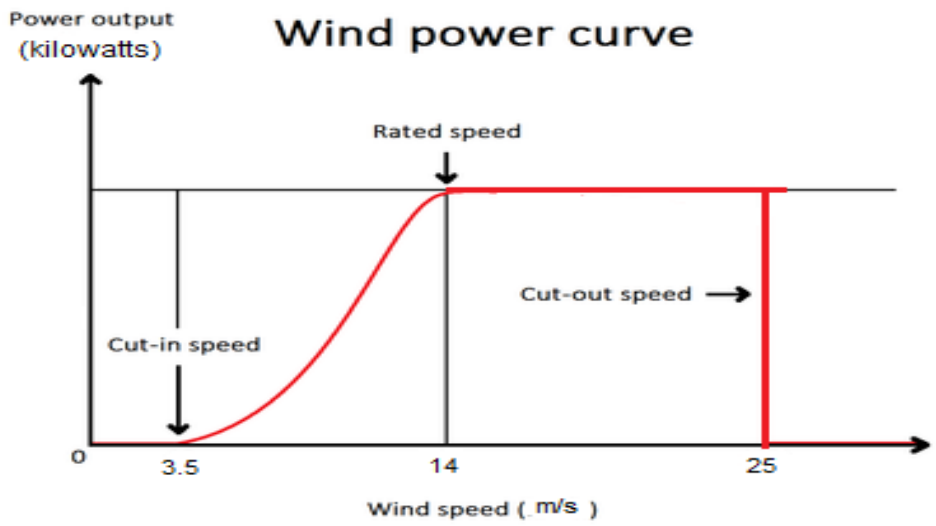

Fig (2.5). The Power Curve, Where Cut-in Speed and Cut-out Speed Is Presented

Turbines are designed to operate within a specific range of wind speeds. The limits of the range are known as the cut-in speed and cut-out speed. The cut-in speed is the point at which the wind turbine is able to generate power. Between the cut-in speed and the rated speed, where the maximum output is reached, the power output will increase cubically with wind speed. For example, if wind speed doubles, the power output will increase 8 times. This cubic relationship is what makes wind speed such an important factor for wind power. This cubic dependence does cut out at the rated wind speed. This leads to the relatively flat part of the curve in Figure (2.5), so the cubic dependence is during the speeds below 15 m/s (54 kph).

The cut-out speed is the point at which the turbine must be shut down to avoid damage to the equipment. The cut-in and cut-out speeds are related to the turbine design and size and are decided on prior to construction. [23, 24]

For example, the site chosen is between (Sabratha and Surman), the average annual wind speed between 10 to 15 m / s which was applied in the simulation model [19].

2.6 GENERATOR

The wind turbine shaft connection fixed with the blades is mechanically connected to the rotor shaft of the generator, so that the mechanical energy developed by the wind turbine as a result of pushing the wind energy (called kinetic energy to circulate into mechanical energy) is transmitted to the shaft. This rotating structure contains a rotor winding (either a field or a motor member). In both cases, we obtain a moving conductor in a static magnetic field or a fixed conductor in a moving magnetic field. In both cases, the voltage is generated by the generator principle. [20-22].

2.6.1 Types of Generators Used In Wind Turbine System

Any types of three-phase generator can connect to with a wind turbine. Several different types of generators which are used in wind turbines are as follows. Asynchronous (induction) generator and synchronous generator. Squirrel cage induction generator (SCIG) and wound rotor induction generator (WRIG) are comes under asynchronous generators. Wound rotor generator (WRSG) and permanent magnet generator (PMSG) are comes under synchronous generator. Detailed explanation is given [24].

2.6.1.1 Asynchronous (Induction) Generator

(a) Squirrel Cage Induction Generator (SCIG)

Squirrel cage induction generator is used for constant speed conditions in this type of wind turbine. The squirrel cage induction motor is connected directly to the wind through the transformer shown in Figure (2.6). There is a capacitor bank here to compensate for reactive power and the soft starter is used for seamless connection to the network. One of its disadvantages is that it does not support any speed control [24].

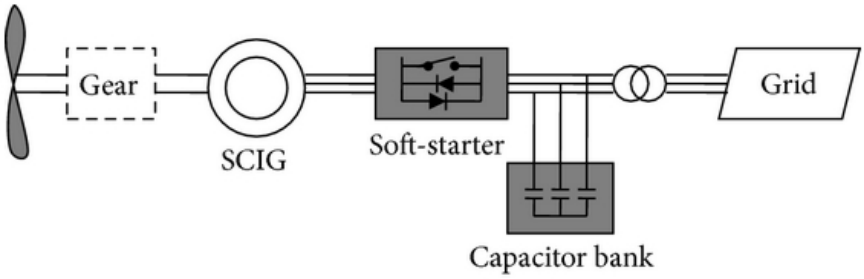

Fig(2.6). Wind Turbine With a Squirrel Cage Induction Generator(SCIG) .

(b) Wound Rotor Induction Generator (WRIG)

In this type (WRIG) the concept of variable speed is used from the turbine and the rotating wound induction generators are directly connected to the network as shown in Figure (2.7). The variable rotor resistance is to control the slip and power output of the generator.

The soft starter used here is used as a reactive power compensator and reducing the current flow to eliminate the demand for reactive power. The speed range is limited, and one of its disadvantages when controlling the active and reactive power is poor, and the slip force dissipates in the variable resistance because it will result in misfits in this configuration [24].

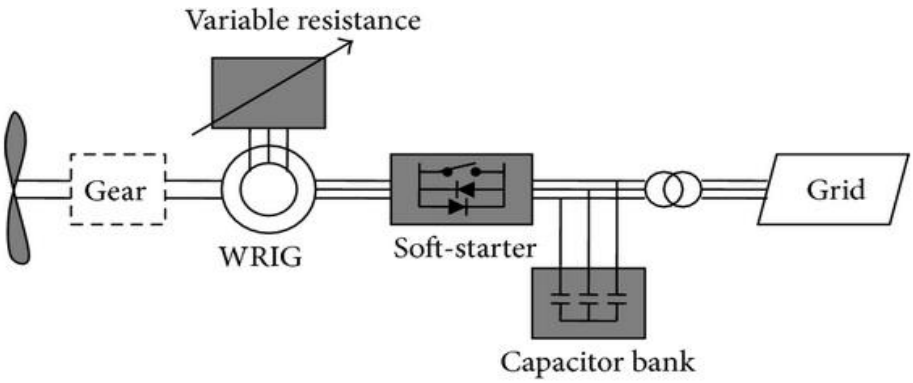

Fig(2.7). Wind Turbine With a Wound Rotor Induction Generator(WRIG).

(c) Doubly Fed Induction Generator (DFIG)

The DFIG consists of a 3 phase wound rotor and a 3 phase wound stator. The rotor is fed with a 3 phase AC signal which induces an ac current in the rotor windings. As the wind turbines rotate, they exert mechanical force on the rotor, causing it to rotate. As the rotor rotates the magnetic field produced due to the ac current also rotates at a speed proportional to the frequency of the ac signal applied to the rotor windings. As a result a constantly rotating magnetic flux passes through the stator windings which cause induction of ac current in the stator winding. Thus the speed of rotation of the stator magnetic field depends on the rotor speed as well as the frequency of the ac current fed to the rotor windings as in the figure (2.8).

The frequency of the rotor ac signal increases as the rotor speed decreases and is of positive polarity and vice versa. Thus the frequency of rotor signal should be adjusted such the stator signal frequency is equal to the network line frequency. This is done by adjusting the phase sequence of the rotor windings such that the rotor magnetic field is in the same direction as the generator rotor [23-25] .

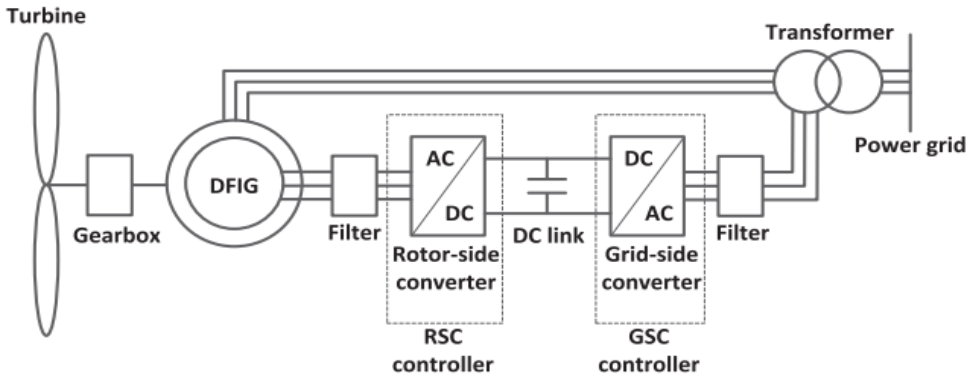

Fig(2.8). Doubly Fed Induction Generator Wind Turbine (DFIG).

2.6.1.2 Synchronous Generator

(a) Wound Rotor Synchronous Generator (WRSG)

Turbine with wound rotor connected to the grid is shown in figure (2.9). This configuration neither require soft starter nor is a reactive power comparator its main advantage. The partial scale frequency converter used in the system will perform reactive power compensation as well as smooth grid connection .

The wide range of dynamic speed control is depends on the size of frequency converter .the main disadvantage is that in the case of grid fault it require additional protection and use slip rings [24].

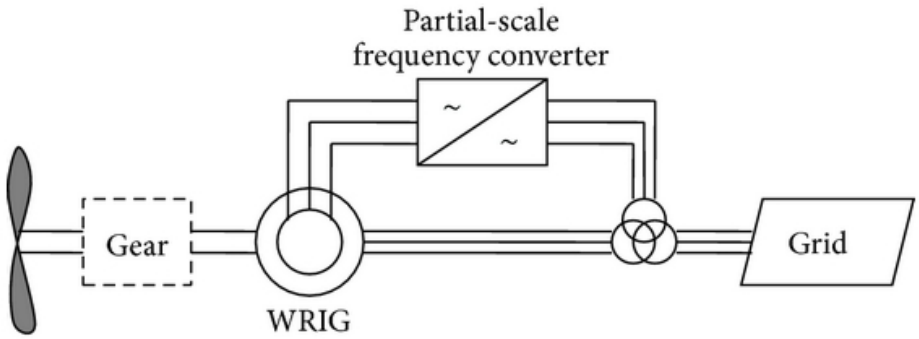

Fig(2.9). Wind Turbine With a Wound Rotor Generator.

(b) Permanent Magnet Synchronous Generator (PMSG)

In this type (PMSG) the generator is connected to the grid via a full range frequency converter shown in figure (2.10) .

A frequency converter helps control both the active and reactive power that the generator supplies to the grid [24].

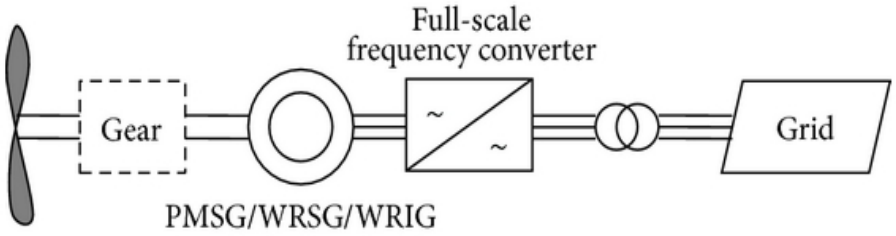

Fig(2.10). Direct-in-line Variable Speed Wind Turbine Connected To The Electric Grid Through a full-Scale Power Converter (PMSG).

2.7 DESIGN CONSIDERATIONS AND CHALLENGES

Generally speaking, wind turbine generators can be selected from commercially available electrical machines with or without minor modifications. If a wind turbine design is required to match a specific site, some key issues should be taken into account. These include [25]:

- Choice of machines.
- Type of drive training.
- Rated and operating speeds.
- Rated and operating torques.
- Tip speed ratio.
- Voltage regulation (synchronous generators).
- Methods of starting.
- Starting current (induction generators).
- Synchronizing (synchronous generators).
- Power converter topology.
- Weight and size.
- Protection (offshore environment).
- Capital cost and maintenance.

2.8 MODELING OF WIND POWER GENERATION UNIT

It is a variable speed, pitch-controlled wind turbine equipped with a double-feed induction generator (DFIG) is the most popular choice for wind power system because it can convert wind energy with high efficiency, control both active and reactive energy, reduce power fluctuations and generate high quality power. Figure (2.11) shows the basic configuration of a grid-connected DFIG wind power system .

The wind turbine is connected to an induction generator through a mechanical shaft system.

The stator of the induction generator is directly connected to the network while the rotor is connected to the network via an AC / DC / AC transformer. A capacitor connected to the DC side acts as a DC voltage source.

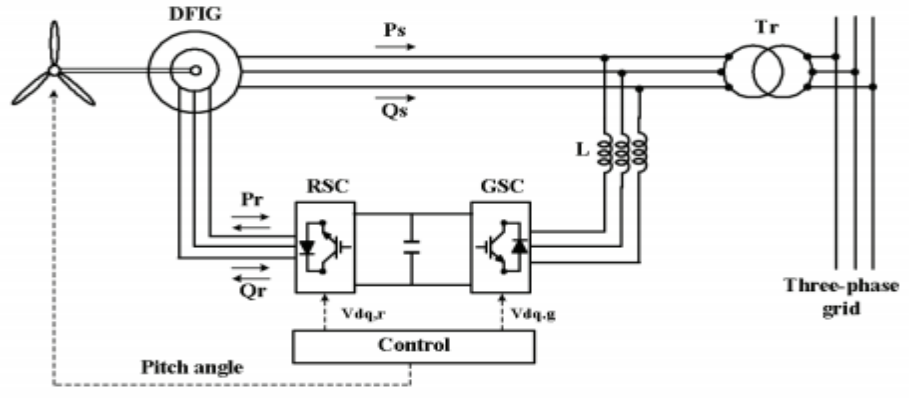

Fig(2.11). Composition Of Wind Conversion System With DFIG

2.8.1 Mathematical Equations of Mechanical Power and Mechanical Torque

The mechanical power extracted from the wind is given by

$$P_m = \frac{1}{2} A\rho V^3 C_p(\lambda, \beta) \quad (2.1)$$

Where ρ =1.225 kg/m3 is the air density, β is the pitch angle, $C_p(\lambda, \beta)$ is the power coefficient, A is the blade's swept area (m^2) and V is the wind speed (m/s). ω_m is angular speed of wind turbine (rad/s) and R is the sweep area radius of the turbine blades, respectively [26-28] .

Where

P_m is mechanical power (W) .

λ is tip speed ratio (TSR) given as = $(\omega_m * {}^{R}/_{V})$.

p is number of poles .

And the mechanical torque developed by the wind turbine shaft is given as

$$T_m = \frac{P_m}{\omega_m} = \frac{1}{2} A\rho V^2 C_p(\lambda, \beta) \frac{R}{\lambda} \quad (2.2)$$

where T_m is mechanical torque (N·m) and R is radius of turbine rotor (m) .

$$C_p(\lambda, \beta) = 0.5176 \left(116 * \frac{1}{\lambda i} - 0.4\beta - 5\right) e^{\frac{-21}{\lambda i}} + 0.0068\lambda \quad (2.3)$$

$$\lambda = (\omega_m * {}^{R}/_{V}) \quad (2.4)$$

Where ω_m is the generator rotating speed. According to Equation (2.4), there is a relation between λ andω_m. At certain wind speed and rotor speed, the power gets maximized and at that instant, rotor speed is called as optimal rotational speed ω_{opt}.This speed corresponds to optimal tip-speed ratio λ_{opt}. So, in order to extract maximum power at variable wind speed condition, the WT should be operated atλ_{opt}.

2.8.2 Model for Shaft System

Figure (2.12) shows a two-mass model for the shaft system [29-31]. It consists of a low-speed wind turbine mass and a high-speed generator mass, neglecting the gearbox mass because of its relatively small inertia .

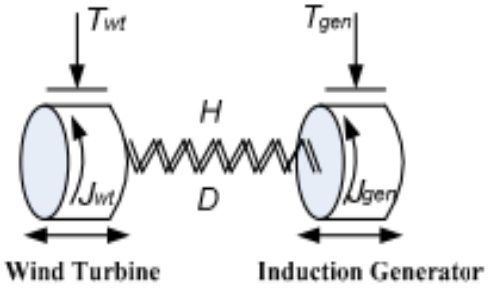

Fig (2.12). Two-Mass Model For The Shaft System Of WTG

The electromechanical dynamic equations are

$$T_{wt} = J_{wt}\frac{d\omega_{wt}}{dt} + D_{wt}(\omega_{wt} - \omega_{gen}) + H_{wt}(\theta_{wt} - \theta_{gen}) \quad (2.5)$$

$$\frac{d\theta_{wt}}{dt} = \omega_{wt} \quad (2.6)$$

$$-T_{gen} = J_{gen}\frac{d\omega_{gen}}{dt} + D_{gen}(\omega_{gen} - \omega_{wt}) + H_{gen}(\theta_{gen} - \theta_{wt}) \quad (2.7)$$

$$\frac{d\theta_{gen}}{dt} = \omega_{gen} \quad (2.8)$$

where ω_{wt} and ω_{gen} are turbine rotational speed and generator rotational speed in *rad/s*, T_{wt} and T_{gen} are turbine torque and generator torque, J_{wt} and J_{gen} are moments of inertia of the turbine and generator respectively, D_{wt} and D_{gen} are linear damping coefficients of the turbine and the generator, H_{wt} and H_{gen} are stiffness coefficients of the turbine and the generator.

2.8.3 The Doubly Fed Induction Generator (DFIG) Model

The DFIG park model in the *d-q* reference frame, assuming sinusoidal flux, constant winding resistance, and neglecting magnetic saturation, is given in figure (2.13) [32-34].

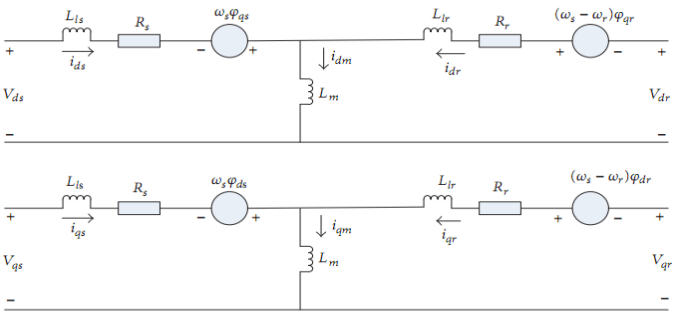

Fig (2.13). DFIG Equivalent Circuit In d-q Reference Frame.

The voltage and flux linkage can be calculated using the following set of equations:

$$v_{ds} = R_s\, i_{ds} - \omega_s\, \varphi_{qs} + \frac{d\varphi_{ds}}{dt} \quad (2.9)$$

$$v_{qs} = R_s i_{qs} + \omega_s \varphi_{ds} + \frac{d\varphi_{qs}}{dt} \quad (2.10)$$

$$v_{dr} = R_r\, i_{dr} - \omega\, \varphi_{qr} + \frac{d\varphi_{dr}}{dt} \quad (2.11)$$

$$v_{qr} = R_r\, i_{qr} + \omega\, \varphi_{dr} + \frac{d\varphi_{qr}}{dt} \quad (2.12)$$

The flux equation are

$$\varphi_{ds} = l_s i_{ds} + l_m\ i_{dr} \quad (2.13)$$

$$\varphi_{qs} = l_s i_{qs} + l_m\ i_{qr} \quad (2.14)$$

$$\varphi_{dr} = l_r i_{dr} + l_m\ i_{ds} \quad (2.15)$$

$$\varphi_{qr} = l_r i_{qr} + l_m\ i_{qs} \quad (2.16)$$

2.8.4 Mathematical Model

Under constant acceleration, the kinetic energy of an object having mass **m** and velocity **v** is equal to the work done, **W** in displacing that object from rest to a distances under a force **F**.

$$E = W = F*s \quad (2.17)$$

According to Newton's Law, we have:

Hence,

$$F = ma \quad (2.18)$$

$$E = ma * s \quad (2.19)$$

Substituting it in equation (2.19), we get that the kinetic energy of a mass in motions is:

$$E = \frac{1}{2} m \upsilon^2 \quad (2.20)$$

$$P = \frac{1}{2} v^2 \frac{dm}{dt} \quad (2.21)$$

$$\frac{dm}{dt} = \rho A v \quad (2.22)$$

Hence, from equations (2.21),(2.22), the power can be defined as:

$$P = \frac{1}{2} \rho A v^3 \quad (2.23)$$

$$A = \frac{\pi d^2}{4} \quad (2.24)$$

$$P = \frac{\pi}{8} \rho d^2 v^3 \quad (2.25)$$

2.8.5 Converter Models

The DFIG is generally used with two back-to-back PWM converters as shown in figure (2.14). The grid-side controller is used to keep the DC-link voltage constant and to make the grid side run at unity power factor, so that no reactive power is flowing between the rotor and the grid. The rotor-side controller allows to control stator voltage and stator active power [30,35,36].

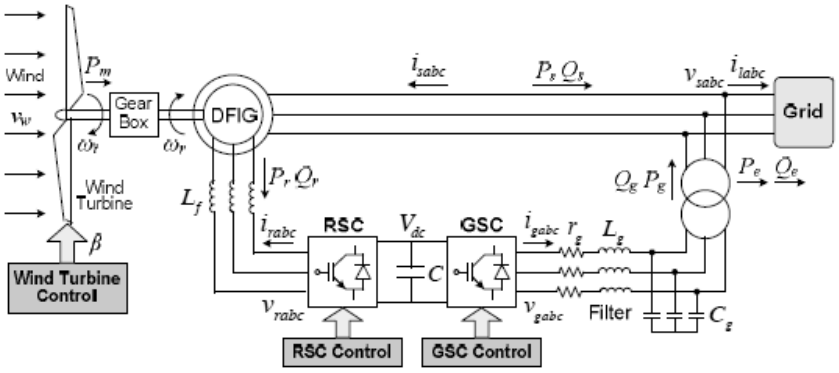

Fig. (2.14). Configuration Of The DFIG With AC DC AC Converter

2.9 CONTROL SYSTEM

2.9.1 Pitch Angle Control System

The pitch angle is kept constant at zero degree until the speed reaches point D speed of the tracking characteristic beyond point D the pitch angle is proportional to the speed deviation from point D speed. For electromagnetic transients in power systems the pitch angle control is of less interest. The wind speed should be selected such that the rotational speed is less than the speed at point D. If wind speed is below the rated value the rotational speed is adjusted so that power coefficient remains max when the pitch angle is zero. Mean while, if wind speed increases above the rated value pitch angle control is activated to increase the pitch angle to limit the mechanical power. Figure (2.15) illustrates a conventional pitch angle control system. [30].

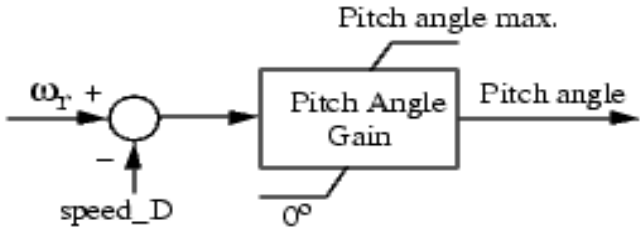

Fig. (2.15). Conventional Pitch Angle Control System.

2.9.2 Control of Rotor Side Converter (RSC)

The stator-voltage oriented reference frame, in which *q-axis* is aligned with stator voltage vector vs is used in rotor-side converter control as shown figure (2.16) [30].

Then, active power and reactive power injected into the grid from the stator terminal are

$$P_s = \frac{3}{2}\left(v_{sd}i_{sd} + v_{sq}i_{sq}\right) = \frac{3}{2}\frac{L_m}{L_s}v_s j_{rq} \qquad (2.26)$$

$$Q_s = \frac{3}{2}\left(v_{sq}i_{sd} + v_{sd}i_{sq}\right) = \frac{3}{2}v_s\left(\frac{v_s}{L_s\omega} - \frac{L_m}{L_s}i_{rd}\right) \qquad 2.27)$$

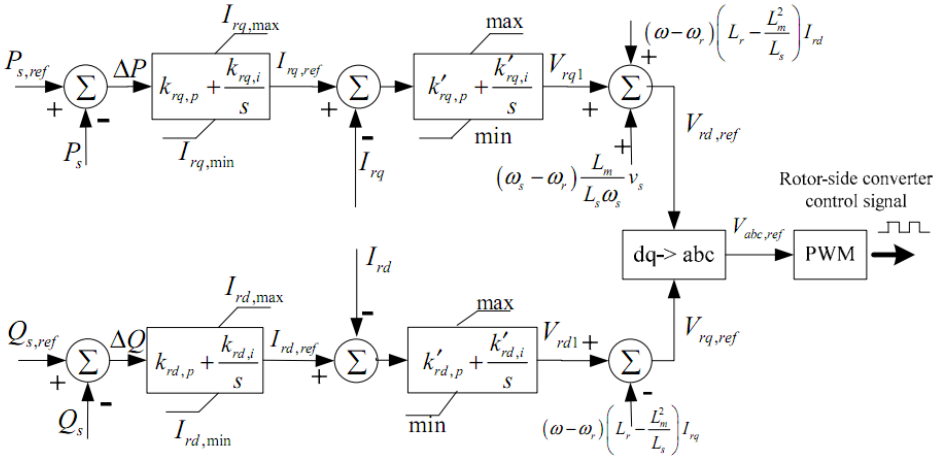

Fig(2.16). Control For Rotor-Side Converter

Consequently, from equation (2.26)(2.27) P_s and Q_s are proportional to $-i_{rq}$ and $-i_{rd}$ respective Thus the equations for the rotating voltage are:

$$v_{rd} = R_r i_{rd} + \left(L_r - \frac{L_m^2}{L_s}\right).\frac{d}{dt}i_{rd} - (\omega - \omega_r)\left(L_r - \frac{L_m^2}{L_s}\right).i_{rq} \qquad (2.28)$$

$$v_{rq} = R_r i_{rq} + \left(L_r - \frac{L_m^2}{L_s}\right).\frac{d}{dt}i_{rq} - (\omega - \omega_r)\left(L_r - \frac{L_m^2}{L_s}\right).i_{rd} + (\omega - \omega_r).\frac{L_m v_s}{L_s\omega} \qquad (2.29)$$

2.9.3 Control of Grid Side Converter (GSC)

The grid-side converter is actually an inverter, and it is controlled in synchronous rotating frame with *d-axis* aligned to the grid voltage vector *($v_{gd}=v_g$, $v_{gq}=0$).* Similar to equation (2.26),(2.27), grid-side active power and reactive power are

$$P_g = \frac{3}{2}\left(v_{gd}i_{gd} + v_{gq}i_{gq}\right) \qquad (2.30)$$

$$Q_g = \frac{3}{2}\left(v_{gq}i_{gd} + v_{gd}i_{gq}\right) \qquad (2.31)$$

From the figure (2.17) Thus P_g and Q_g are proportional to i_{gd} and $-i_{gq}$, respectively . Active power can be represented in terms of capacitor voltage v_{dc}, so by regulating i_{gd} and i_{gq} capacitor voltage and grid-side reactive power can be controlled. Using a *PI* controller, the reference values for the controlled currents are

$$i_{gd,ref} = \left(K_P + {}^{K_i}/_{S}\right).\left(V_{dc.ref} - V_{dc}\right) \quad (2.32)$$

$$i_{gq,ref} = \left(K_P + {}^{K_i}/_{S}\right).\left(Q_{gc.ref} - Q_g\right) \quad (2.33)$$

The relation between voltage v_s and v_g *is*

$$v_{sd} = v_{gd} + R_g i_{gd} + L_g.\frac{d}{dt} i_{gd} - \omega L_g i_{gq} \quad (2.34)$$

$$v_{sq} = v_{gq} + R_g i_{gq} + L_g \frac{d}{dt} i_{gq} + \omega L_g i_{gd} \quad (2.35)$$

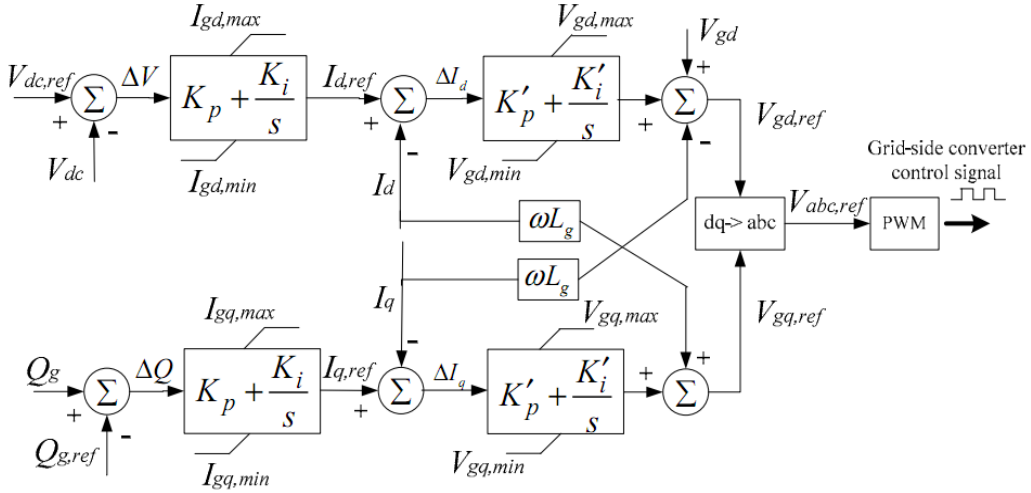

Fig(2.17). Control For Grid-Side Converter

2.10 GRID SYNCHRONIZATION

One of the most important aspects of DG (Distributed Generation) systems is the grid synchronization.

While synchronizing a DG with a utility grid it shall not cause a voltage fluctuation of more than ± 5% of the existing voltage level at the Point of Common Coupling (PCC).

The injected current into the utility network has to be synchronized with the grid voltage. Therefore, grid synchronization algorithms play an important role for distributed power generation systems.

The synchronization algorithm mainly outputs the phase of the grid voltage vector which is used to synchronize the control variables. The most important primary method in discovering network imbalance[34,35].

1- Zero-Crossing Method.

2- αβ and dq Filtering Algorithm .

3- Phase-Locked-Loop (PLL).

2.10.1 Zero-Crossing Method

In the zero-crossing method, the phase angle of the grid is determined according to the time difference between two zero-crossing points of the grid voltage. Since the zero-crossing points are only updated at every half cycle of the utility voltage frequency, the dynamic performance of this technique is low. Other than zero-crossing delay, an additional filtering has to be applied in order to detect the fundamental frequency, which introduces extra delay to the system. Filtering delay can be improved by using special high order predictive filters without delay, but these filters add more complexity to the system. Among all technique, the zero crossing method has the simplest implementation, but also poor performances are reported when using it, mainly if grid voltages register variations such as harmonics or notches.

2.10.2 αβ And dq Filtering Algorithm

The grid phase angle can be obtained by filtering the grid voltage in stationary (αβ) or synchronous (dq) frames. Figure (2.18) shows the schematic of these methods of synchronization.

As can be seen, the phase angle of the grid is extracted using filtering in either stationary or synchronous frame. In stationary frame, the arc-tangent function is directly applied to the frame but in synchronous frame, the dq signal must be transformed back into the stationary frame before applying the arc-tangent function. The drawback of this method is the use of filtering, which introduces a delay to the system, and therefore the calculated phase angle will lag the real phase angle.

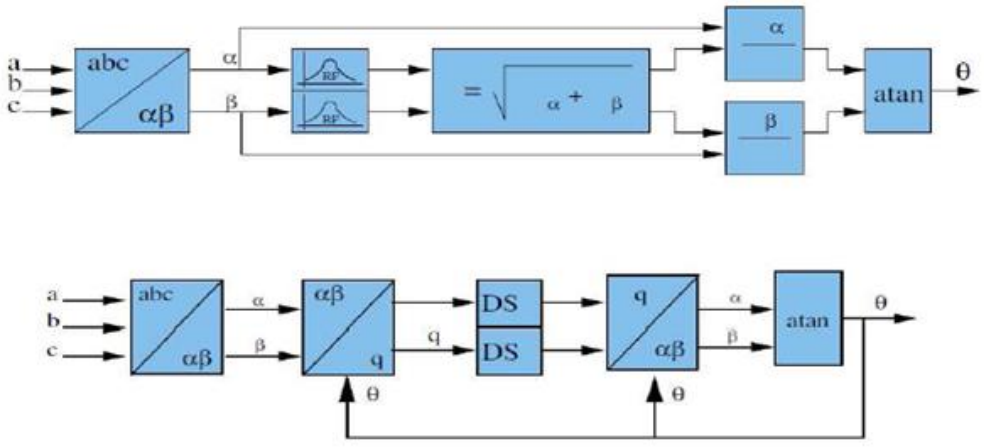

Fig(2.18). Synchronization Method Using αβ And dq Frames

2.10.3 Phase-Locked-Loop (PLL)

The third method of synchronization is the phase-locked-loop technique, which is the method that will be used because it is appropriate and works for the purpose. A basic PLL circuit often consists of three essential components: a phase detector, a loop filter, and a Voltage Controlled Oscillator (V_{CO}). Using a negative feedback loop, PLL minimizes the phase and frequency errors between the input and output signals. Frequency is the time derivative of phase. Keeping both the input and output phase in lock step implies keeping the input and output frequencies in lock step. Consequently it can track an input frequency or it can generate a frequency that is a multiple of the input frequency. The schematic of PLL is depicted in Figure (2.19). This algorithm has better harmonic and disturbance rejection compared to zero-crossing and αβ-dq transformation, but during grid unbalance conditions, this algorithm requires further improvements.

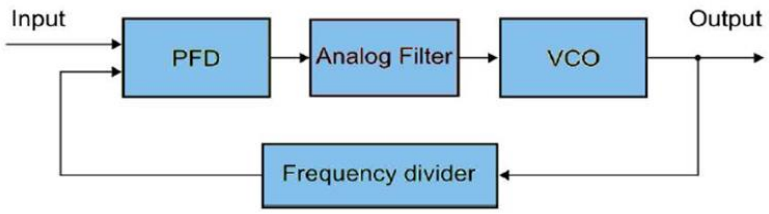

Fig(2.19) Phase-Locked-Loop Scheme

More details regarding the concept and implementation of this synchronization technique can be found in literature. Because of its advantages and wide practical usage, PLL technique will be employed in the simulation of the wind turbine system in this thesis.

2.10.3.1 Synchronous Reference Frame (SRF) PLL

In the conventional PLL, three-phase voltage vector is translated from the abc natural reference frame to the αβ stationary reference frame by using Clarke's transformation, and then translated to dq rotating frame by Park's transformation as shown in Figure (2.20). The angular position of this dq reference is controlled by a feedback loop which makes the q-axis component equal to zero in steady state. Therefore, under steady state condition, the d-axis component will be the voltage vector amplitude [36].

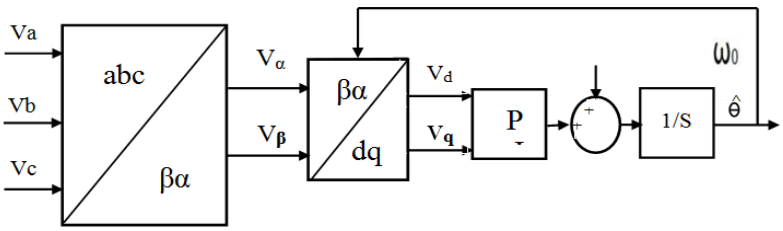

Fig(2.20). Basic Block Diagram Of The Conventional PLL

2.11 WIND TURBINE ROTOR SIZES

From equation (2.36) to that the available energy is proportional to the square of the rotor diameter, as well as with the cube of the wind speed.

Therefore, to keep everything else constant, the power increase is proportional to the square of the ratio of the increased diameter to the initial rotor diameter:

$$\frac{P(d)}{P_0(d)} = \left(\frac{d}{d_0}\right)^2 \qquad (2.36)$$

According to Enercon's design for 2014(http://www.enercon.de), a 15 KW wind turbine will have a rotor diameter of 5.6 meters, which is taken as a reference as shown Table (2.1) .

TABLES 2.1: The Generator Rated Power As A function Of Rotor Diameters

Rotor diameter(m)	Generator rated power (kw)
3.3	5
5.6	**15**
11	50
15	100
36	600
46	1000
127	7500

2.12 WIND TURBINE POWER COEFFICIENT (C_P)

(C_p) is the ratio of actual electric power produced by a wind turbine divided by the total wind power flowing into the turbine blades at specific wind speed.

Betz' Law. The theoretical maximum power efficiency of any design of wind turbine is 0.59 (i.e. no more than 59% of the energy carried by the wind can be extracted by a wind turbine). This is called the "power coefficient" and is defined as:

$$C_P = \frac{\textbf{Actual Electrical Power Produced}}{\textbf{Wind Power into Turbine}} = \frac{P_{Out}}{P_{in}} \qquad (2.37)$$

C_p *max = 0.59*

Wind turbines cannot operate at this maximum limit. The C_p value is unique to each turbine type and is a function of wind speed that the turbine is operating in. Once we incorporate various engineering requirements of a wind turbine - strength and durability in particular – the real world limit is well below the Betz Limit with values of 0.3 - 0.4 common even in the best designed wind turbines. By the time we take into account the other factors in a complete wind turbine system .e.g. the gearbox, bearings, generator and so on - only 10-30 % of the power of the wind is ever actually converted into usable electricity. Hence, the power coefficient needs to be factored in equation (2.38) and the extractable power from the wind is given by [27]**:**

$$P_{avail} = \frac{1}{2}\rho A \upsilon^3 C_p \qquad (2.38)$$

2.13 CALCULATIONS WITH GIVEN DATA

The data of the system is given as following:

Actual Electrical Power Produced, $P_{Out} = 15\ Kw$

Rotor Blade dimeter, $d = 5.6\ m$

Wind speed, υ *= 15 m/sec*

Air density, ρ *= 1.225 kg/m3*

Inserting the value for blade length as the radius of the swept area we have:

$$r = \frac{d}{2} = \frac{5.6}{2} = 2.8\ m$$

$$A = \pi r^2$$

$$A = \pi(2.8)^2 = 24.6\ m$$

Then, the power Coefficient (C_p) from the wind into rotational energy in the turbine can be calculated by using equation:

$$C_P = \frac{P_{Out}}{\frac{1}{2}\rho A \upsilon^3} = \frac{15000}{\frac{1}{2} \times 1.225 \times 24.6 \times 15^3} = 0.3$$

This value is used for the designed model, than normally defined by the turbine designers but it is important to understand the relationship between all of these factors and to use this equation to calculate the power Coefficient.

2.14 SIZING & SPECIFICATION OF THE DESIGNED SYSTEM

In this design production of a total power of 60 kw divided into four turbines and for each turbine 15 kw, relys on wind turbines so that the diameter of the turbine blades is 5.6 m and the height of the turbines on the ground is about 80 meters at wind speeds from 10 to 15 m / s and this is done by the turbine designers to determine the Values From here, we notice that the higher the turbine rises, the higher its speed, and thus we raise the turbine to a certain distance from the surface of the earth (80 meters) to produce the required speed (10-15 m / s) **(based on Measurements of the nature of weather conditions in Libya and the area between Surman and Subratha)**.

Attention to the overload power and efficiency of the AC DC inverter. Depending on the climate and the efficiency of the AC DC inverter connected to the network at figure (2.21) it is expected to obtain an average of up to 90% of the nominal classification of the wind turbines and to maintain that no electrical noise is produced to avoid its interference with the waves of electronic devices. It is very important to turn off the operation when any malfunction in the network for the safety of engineers and technicians to repair the malfunction.

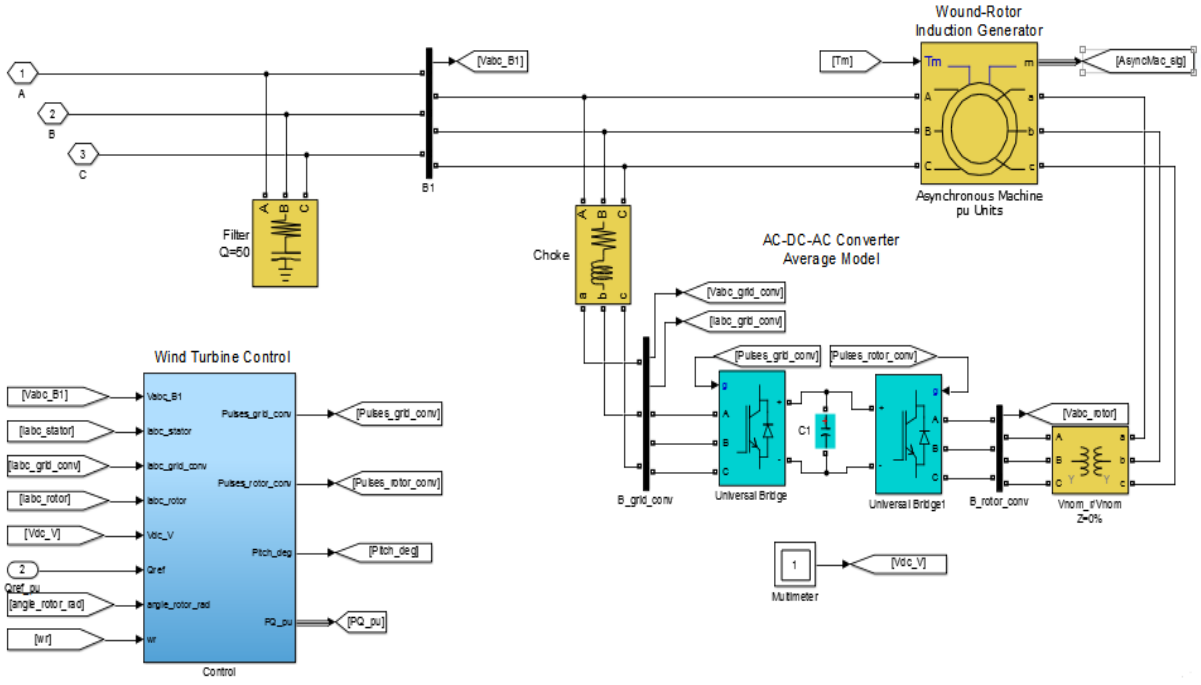

Fig (2.21) Grid-Connected AC DC AC Converter

Sizing and specifications of the designed system to power plant are presented in Tables 2.2

TABLES 2.2: Wind Power Plant Specification

Wind power plant specifications	
Rated power plant	60 kw
Rated power turbine	15 kw
Voltage output	390 v
Nominal mechanical output power	1.5e4 w
No of turbine	4
Frequency	50 Hz
Wind panal specification	
TYPE	HAWT
No of blades	3
Rated of blades	15 Kw
Power coefficient	Cp=0.3
Reted wind speed	15 m/s
DFIG generator specifications	
Input Stator voltage Vs nom(Vrms)	575V
Input rotor voltage Vr nom (Vrms)	800V
Stator Resistance and inductance	[0.023 0.18] pu
Rotor Resistance and inductance	[0.016 0.16]
Magnetizing inductance Lm	2.9 pu
Nominal Output Current	56 A
Max. Output Current	76 A
Nominal AC Output Voltage	400Vac
AC OutputVoltageRange	360 – 440 Vac
Power Factor (cosφ)	0.9(Lead) ~ 0.9(Lag)
Max.efficiency	96.8 %
Operating Temperature	25Co - +60Co
Grid specifications	
Number of phases	3-phases
Voltage rating	380 volts
Frequency	50 Hz
Number of phases	3-phases

C H A P T E R THREE

PHOTVOLTAIC CELL (PV)

3.1 INTRODUCTION

Solar energy is the process of converting light (photons) into electrical voltage because solar photovoltaic cells convert sunlight directly into solar energy (electricity). They use thin layers of a semiconductor material that has a different charge between the upper and lower layers. When exposed to daylight, the electrons in the semiconducting material absorb the photons, increasing their activity and the movement of electrons generates a current known as direct current (DC).

3.2 PHOTVOLTAIC (PV) ENERGY

A photovoltaic energy system is mainly powered by solar energy. The configuration of PV system is manifested in figure (3.1). It contains PV modules or arrays, which convert solar energy in the form of solar irradiation into electric energy .The dc-dc converter changes the level of the voltage to match it with the electrical appliances that are supplied by this system [37] .

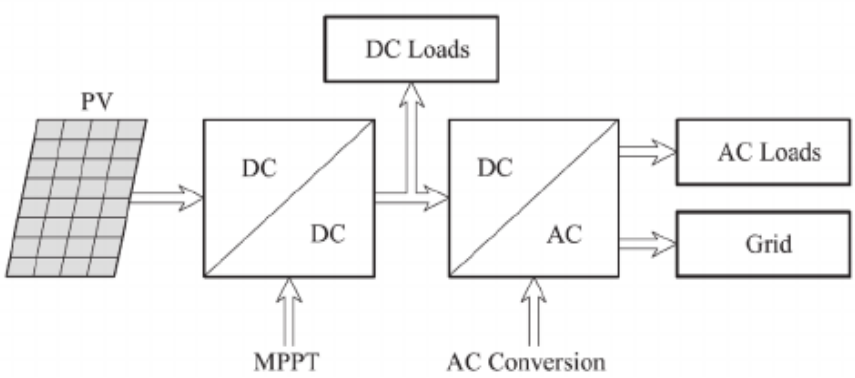

Fig (3.1). Overall Block Diagram Of PV Energy System

This DC-DC converter may be either buck or boost or buck-boost contingent on the required and available voltage levels. The maximum power point Tracing system coerces the maximum power from the PV modules.

A bi-directional converter which is able to supply the current in both the directions is used to charge the battery when there is a power surplus and the energy stored by the battery is discharged into the load when there is a power deficit.

3.3 SOME ADVANTAGES AND OF PV SYSTEMS

3.3.1 Advantage of Solar PV System

1. PV panels produce neat – green energy .
2. Cost of solar panels has fallen considerably in recent years thereupon future of solar PV panels is indeed bright for environmental sustainability and economical viability .
3. PV systems can supply electricity in locations where electricity distribution systems (power lines) do not exist, and they can also supply electricity to an electric power grid.
4. Maintenance and operating costs are considered to be less, nearly negligible, as compared to other sources .
5. PV panels are totally soundless.
6. Residential solar panels are can be simply set up on the ground or on rooftops without any interference to residential lifestyle.

3.3.2 Disadvantage of Solar PV System

1. As in the case of all renewable energy sources, solar energy has regularity problem .
2. They need extra devices for converting DC to alternating electricity AC so that it can be used on the distribution system .
3. To get an uninterrupted provision of electric power, for some applications storage batteries are also required; that increases the cost.
4. Although they have no significant operating costs or maintenance costs, they are delicate and can be tampered relatively easily.

3.4 TYPES OF SOLAR CELLS

There are many ways to manufacture solar cells and accordingly there are different types of these cells, all of which perform the same function, which is converting light into electricity, but they differ in efficiency, cost and some details, and the most important types of these cells [38].

a. Monocrystalline Solar Cells

This type is highly pure, and the most efficient among the types of solar cells, it is produced from a single crystal and therefore has a single molecular model, and has a distinctive appearance, the efficiency of this type is about 16%, but it is very expensive as shown figure (3.2)[38].

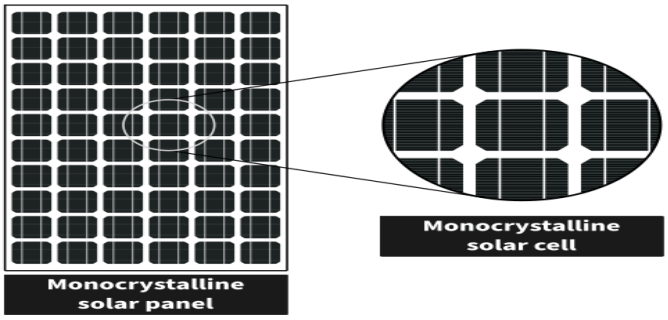

Fig(3.2). Monocrystalline Solar Cells

b. Polycrystalline Solar Cells

This type of cell is manufactured by melting silicon and pouring it into special molds to give it the desired shape, and this process will result in a polycrystalline model with different directions and shapes, its efficiency ranges from 9% to 13%, and its cost is medium, which makes it suitable for commercial use as shown figure (3.3)[38] .

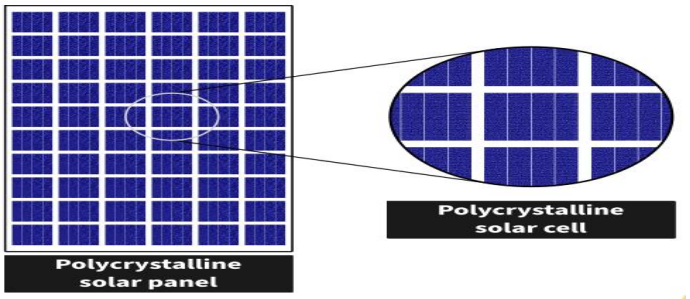

Fig(3.3). Polycrystalline Solar Cells

c. Thin Film Solar Cells

The biggest differentiating aesthetic factor when it comes to thin-film solar panels is how thin and low-profile the technology is. As their name suggests, thin-film panels are often slimmer than other panelty They are considered to be the lowest in terms of efficiency ranging from 3% to 6% and low cost, due to their relatively easy manufacturing method; Where silicon is deposited on glass or plastic surfaces, solar cells are formed as shown figure (3.4) [38].

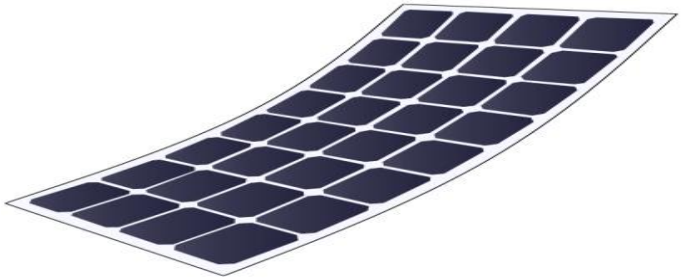

Fig(3.4). Thin Film Soler Cells

3.5 PHOTOVOLTAIC ARRANGEMENTS

3.5.1 PV Cell

When shining a light on the solar cell (PV), part of the radiation is reflected and the other part is absorbed or passed through the solar panels made of semiconducting materials (which have a positive charge and a negative charge) as shown in figure (3.5).

A cellular semiconductor material is defined as the difference between two energy levels: the valence band and conduction band. The low-energy valence band contains negatively charged electrons, while the high-energy conduction band is blank. When the photons hit the electrons with an energy greater than the band gap, they can absorb enough energy to stimulate them from the valence band to the conduction band. N-type) and other fraction with electron receptors (p-type doping) creating a p-n junction [37] .

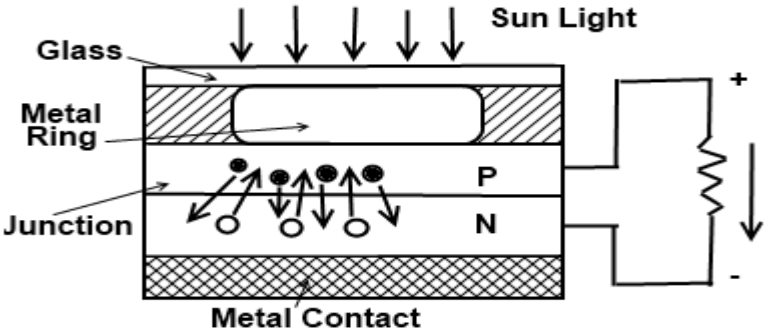

Fig (3.5). Structure Of PV Cell

3.5.2 PV module

A single cell generate very low voltage (around 0.4) , so more than one PV cells can be connected either in serial or in parallel or as a grid (both serial and parallel) to form a PV module as shown in figure (3.6).

When we need higher voltage, we connect PV cell in series and if load demand is high current then we connect PV cell in parallel. Usually there are 36 or 76 cells in general PV modules. Module we are using having 36 cells.

The front side of the module is transparent usually build-up of low-iron and transparent glass material, and the PV cell is encapsulated. The efficiency of a module is not as good as PV cell, because the glass cover and frame reflects some amount of the incoming radiation [39, 40].

3.5.3 PV array

A photovoltaic array (PV system) is an interconnection of modules which in turn is made up of many PV cells in series or parallel. The power produced by single module is not enough to meet

the requirements of commercial applications, so modules are connected to form array to supply the load. In an array the connection of the modules is same as that of cells in a module shown figure (3.6) [41] .

The modules in a PV array are usually first connected in series to obtain the desired voltages; the individual modules are then connected in parallel to allow the system to produce more current. In urban uses, generally the arrays are mounted on a rooftop [38].

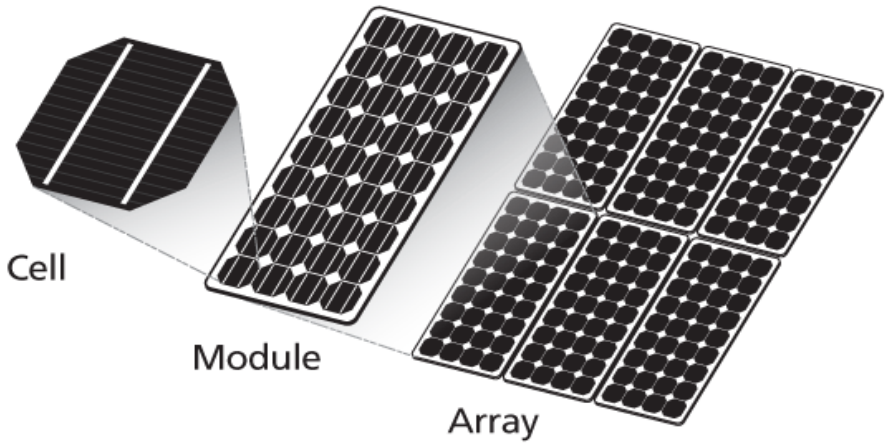

Fig (3.6) Photovoltaic System

In this work the monocrystalline PV modules from Sun power were selected because they are more space-efficient, higher heat tolerance, longer life span than the others and they tend to be more efficient.

The following table represents the datasheet of selected monocrystalline module for system design and that provided by the manufacture which will modelled and simulated to compare it is response to the datasheet information which illustrated in table Full details for selected module specification include. Typically, three points (I_{sc}, 0), (V_{oc}, 0) and (V_{mpp}, I_{mpp}) are provided by the manufacturer's datasheet at Standard Test Conditions (STC) as tables 3.1.

TABLES 3.1: Standard Test Conditions (STC)

Solar panel specifications	
Maximum Power (Pmax)	220 W
Voltage at Pmax (Vmp)	41.0 V
Current at Pmax (Imp)	5.37 A
Open-circuit voltage (Voc)	48.6 V
Short-circuit current (Isc)	5.75 A
Temperature coefficient of Isc	3.5 mA/^{o}C
Temperature coefficient of Voc	-132.5mV/^{o}C

3.6 SOLAR CELLS WORK PRINCIPLE

The solar cells are placed directly under the sun. So that its rays are absorbed and converted directly into electrical energy, so that this energy benefits the human being in all areas of his life.
When a semiconductor material absorbs light, the material's electrons begin to be emitted. This happens because the light is composed of small energizing particles called photons, after receiving energy from sunlight, the semiconductor electrons get excited and jump to the conduction bar from the valence band and are free to move, the particles move in only one direction and the current develops. Semiconductor materials contain metal electrodes through which the current exits, which causes the release of electrons from silicon (a semiconductor material) until they are collected in the form of solar energy, as in Figure (3.7)[37].

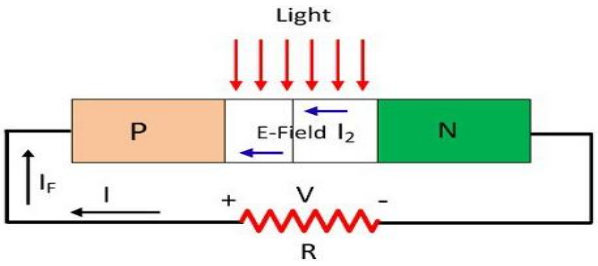

Fig (3.7) Working Of PV Cell

3.7 MODELLING OF PV CELL

Although PV systems have many advantages, they have suffered from changing system performance due to weather changes (solar irradiance, temperature) figure (3.8), high installation cost, and low efficiency that does not reach 20 % per unit [42].
Therefore, PV system modelling is an important aspect of improving the performance of PV systems and there are mathematical equations for PV modules individually.

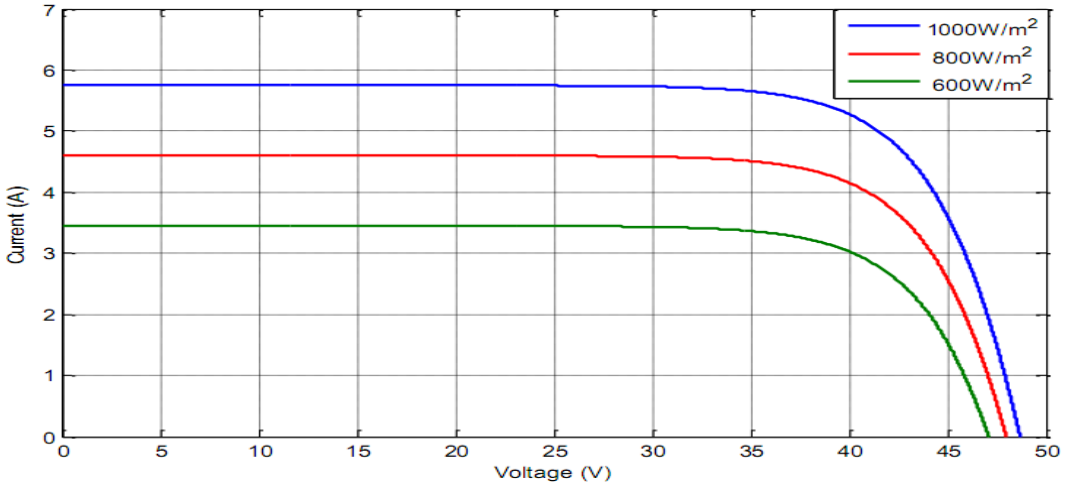

(a) : I-V Characteristic With Varying G From 600 to 1000 At Constant Temperature

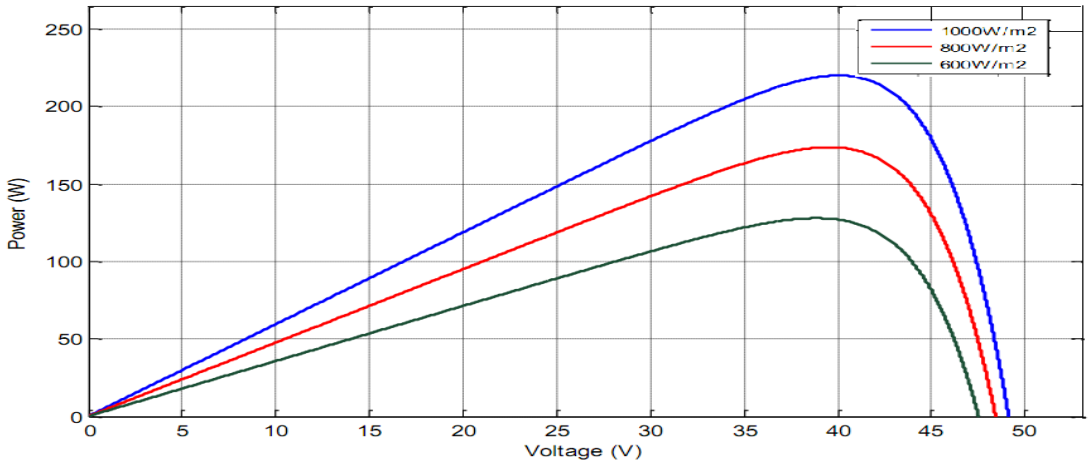

(b): P-V Characteristic with Varying G from 600 to 1000 at Constant Temperature

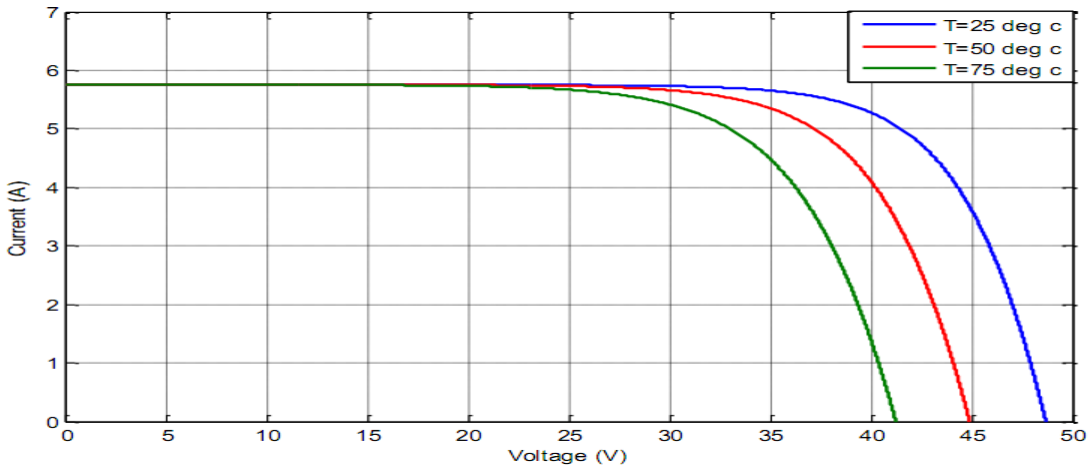

(c): I-V Characteristic With Varying T From 25^{o}C to 75 ^{o}C At Constant Irradiation

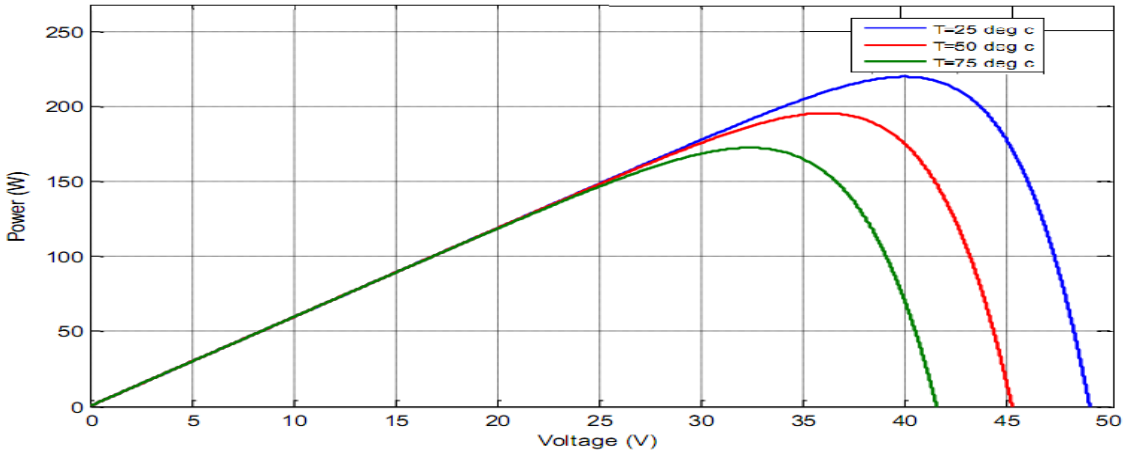

(d): P-V Characteristic With varying T from 25 ^{o}C to 75 ^{o}C At Constant Irradiation

Fig (3.8) (a,b,c,d). Weather Change Curve For IV, PV Solar Radiation, Temperature.

From the Figure (3.9) shows and in series / parallel as they are connected in a PV system. Figure (3.10) shows a PV array, consisting of multiple modules, linked in series and parallel [43, 44].

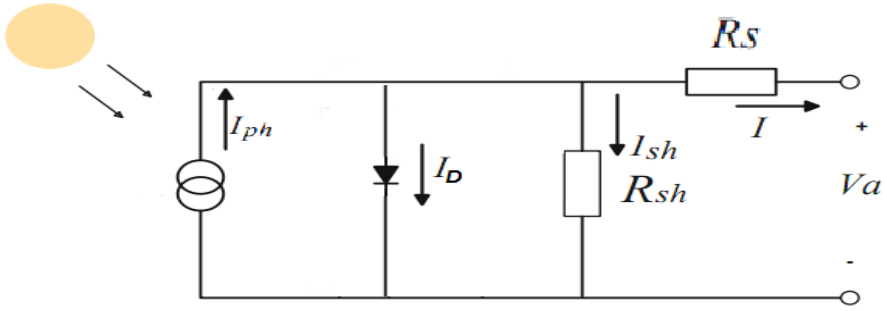

Fig (3.9) . Equivalent Circuit Of Single Diode Modal Of a Solar Cell

The PV cell can be modelled as a diode in parallel with a constant current source and a shunt resistor. These three components are in series with the series resistor as shown figure (3.9)[45] . The output terminal current (I) is equal to the light generated current (I_{ph}), less than the diode current (I_D) and the shunt-leakage current. (I_{sh})

$$I = I_{ph} - I_D - I_{sh} \tag{3.1}$$

Where *Va* is the terminal voltage of the cell .

The diode current is given by the classical diode current expression .

$$I_D = I_d \left[\frac{qV_a}{AKT} - 1\right] \tag{3.2}$$

Where I_D = the saturation current of the diode

q = the electron charge = $1.6 * 10^{-19}$ Coulombs

A = described as the ideality factor of the diode and its value is between 1 and 2

K = Boltzmann constant =$1.38 * 10^{-23}$ Joule/°KT

T = temperature [°K]

The load current is given by the expression :

$$I = I_{ph} - I_{os}\left\{exp\left[\frac{qV_a}{AKT}\right] - 1\right\} - \frac{V_a}{R_{sh}} \tag{3.3}$$

Where

$$I_{ph} = [I_{SC} + K_I\,(T - 25)]\frac{G}{1000} \tag{3.4}$$

$$I_s = I_{or}\left(\frac{T}{T_r}\right)^3 \exp\left[\frac{qE_{GO}}{AK}\left(\frac{1}{T_r} - \frac{1}{T}\right)\right] \tag{3.5}$$

Efficiency of a PV cell does not depend on the variation in the shunt resistance R_p of the cell but efficiency of a PV cell greatly depends on the variation in series resistance R_s. As R_p of the cell is inversely proportional to the shunt leakage current to ground so it can be assumed to be very large value for a very small leakage current to ground. As the total power generated by a single PV cell is very low, we used a combination of PV cells to fulfill our desired requirement. This grid of PV cells is knows as PV array. [43,44].

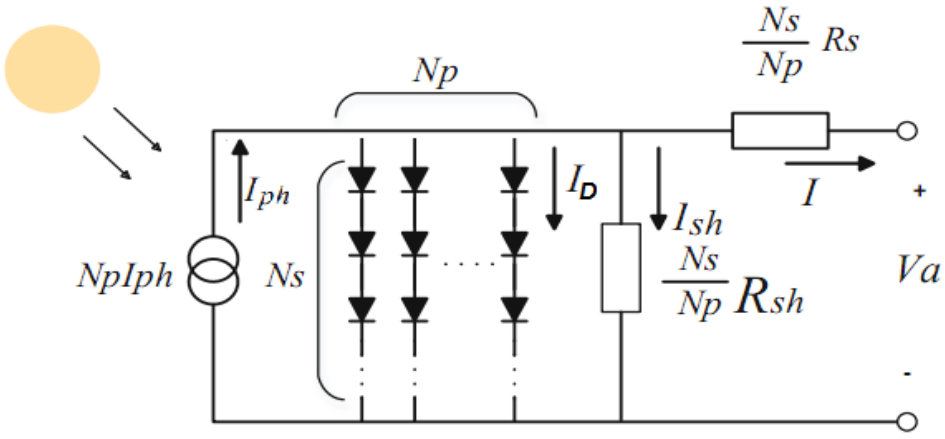

Fig (3.10). Equivalent Circuit Of PV Arry

$$R_{s,arry} = \frac{N_s}{N_p} R_s \tag{3.6}$$

$$R_{sh,arry} = \frac{N_s}{N_p} R_{sh} \tag{3.7}$$

$$I = I_{ph} N_P - I_D N_P \left[exp\left(\frac{q}{AKT} \left(\frac{V_a}{N_S} + \frac{IR_S}{N_p} \right) \right) - 1 \right] \left[\frac{V_a}{N_s} + \frac{IR_s}{N_p} \right] \tag{3.8}$$

Small change in chain resistance can further affect PV cell efficiency but difference in shunt resistance does not affect more. For a very small leakage current to the ground, the mathematical equation of the model can be expressed as follows.

$$I = I_{ph} N_P - I_D N_P \left[exp\left(\frac{q}{AKT} \left(\frac{V_a}{N_S} + \frac{IR_S}{N_p} \right) \right) - 1 \right] \tag{3.9}$$

Where;

I,V_a cell output current and voltage and

R_s series resistance .

I_{os} cell reverse saturation current .

K_I short circuit current temperature coefficient at I_{SCR} , K_I = 0.0017 A/℃ .

G solar irradiation in W/m^2.

I_{SCR} short circuit current at 25° C and 1000 W/m^2.

I_{ph} light generated current

E_{GO} band gap for silicon .

T_r reference temperature, Tr =301.18° k.

I_{or} cell saturation current at T_r and R_{sh} = shunt resistance.

N_P Number of parallel cells.

N_S Number of series cells.

I-V and P-V characteristics of PV module are shown in figure (3.11), respectively.

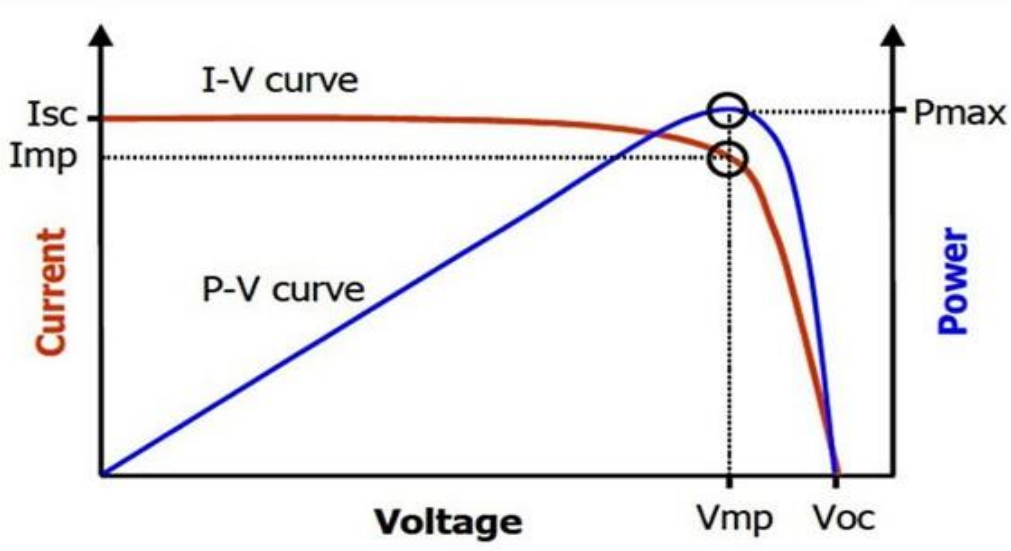

(a)

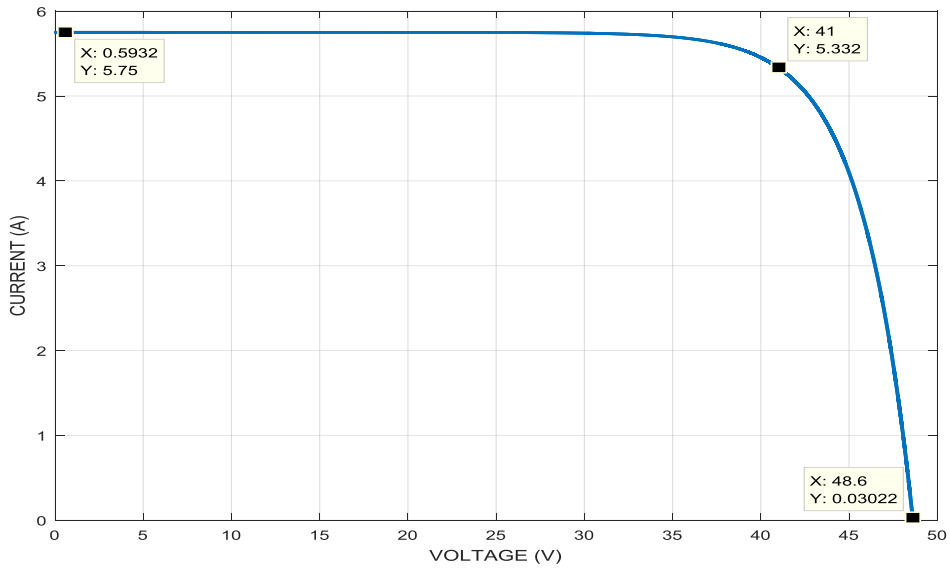

(b)

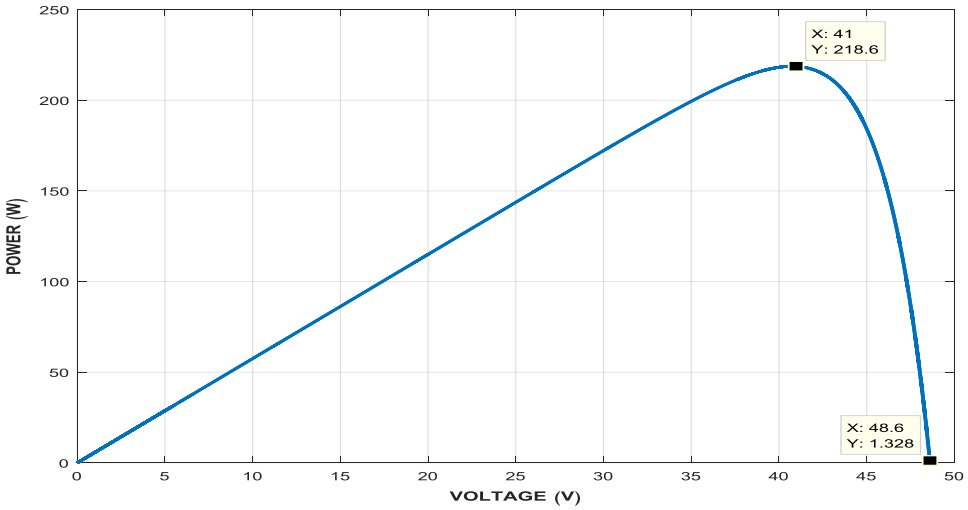

(c)

Fig (3.11). **(a)**The typical I-V and power-voltage (P-V) Curves are based on the cell model; P_{max} is the maximum power point, while I_{mp} is the current and Vmp is the voltage at the maximum power point. Characteristic **(b)** I-V and **(c)** P-V curves of a solar panel.

Depending on the load energy demand per day, energy produced by PV system during the day, certain ratio of average daily energy consumption is considered as essential loads and is target by supplying energy from PV system during day perio [45] .

when electric main supply on and off, so this type of operation may reduce bill value dramatically. The total value of the DC current and voltage that produced from the whole PV system can be calculated by using rated module voltage Vmpp, rated module current Impp, and the number of modules in series-parallel connection respectively as shown the tables (3.1) [46].

$V_{dc(total)} = V_{mpp}$ x (No of series connected modules) (3.10)

= 41 x 10 = 410 V

$I_{dc(total)} = I_{mpp}$ x (No of parallel connected modules) (3.11)

= 5.37 x 40 = 214.8 A

$P_{dc(total)} = I_{dc(total)} \times V_{dc(total)}$ (3.12)

= 410 x 214.8 = 88 kw

After investigation of the whole system I-V and P-V characteristics, rated output DC voltage and current it found accurately validate to the information provided by the manufacture's data sheet and theory calculation.

In Figure (3.12) shows the simulation results for I-V and P-V characteristics respectively of the PV panel with output roughly of 88 KW at standard test condition with specifying current and voltage values of the system at maximum power point.

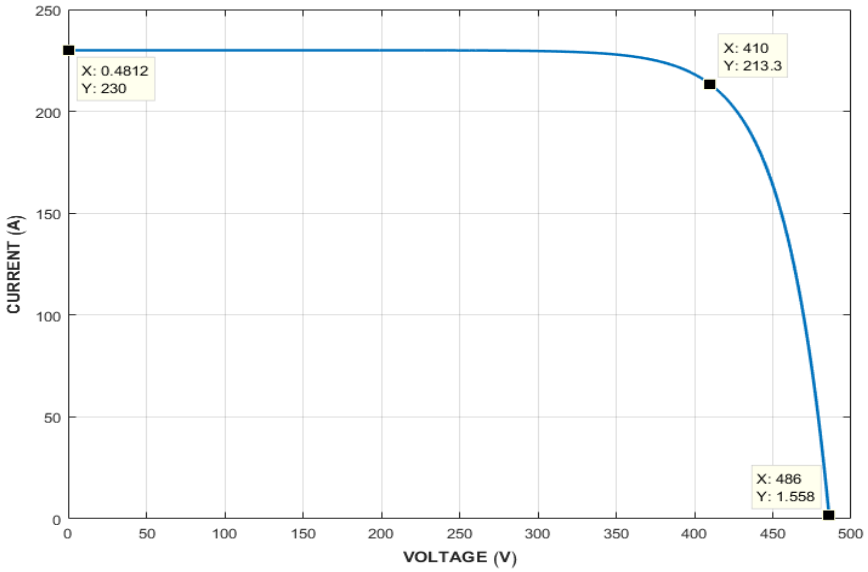

(a)

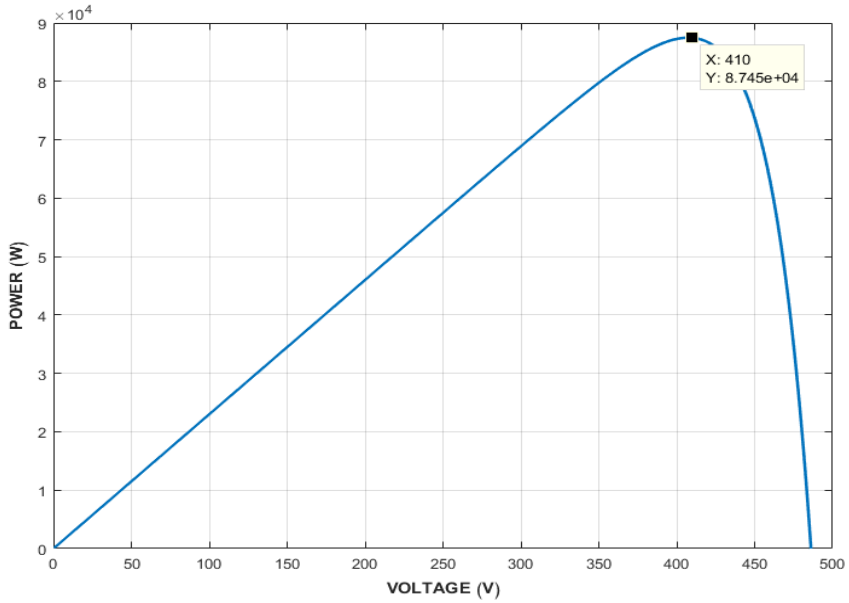

(b)

Fig (3.12).(a) I-V and (b) P-V . Characteristics Respectively Of The PV Panel

3.8 SHADING EFFECT

When a unit or part of it is shaded, it begins to generate less voltage or current compared to the unit not shaded. When the units are connected in series, the same current will flow in the whole circuit but the shaded part cannot generate the same current but must allow the same current to flow, so the shaded part will start acting like a load and start to consume power As in the following figure (3.13) [47] .

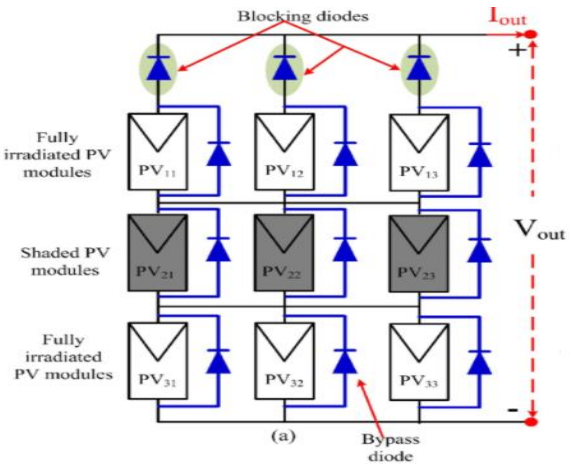

Fig (3.13) PV Array in Shaded condition

When the shaded portion begins to act as a load, this condition is known as the hotspot problem. Without proper protection, the problem of hot spots may arise, and in severe cases, the system may be damaged. To reduce the damage in this case, a bypass diode can generally be used.

Thus when the shaded shade current flows through the bypass diode instead of the shaded series because the side diode is directly biased, and as a result, no energy is lost in the shaded cells and the illuminated cells generate only energy.

And thus, Figure. (3.14) shows the effect of bypass diodes on PV properties of the PV panel and multiple peaks may occur on the curve and thus the conventional MPPT algorithms are unable to track the global peak which is the true MPP [38,41].

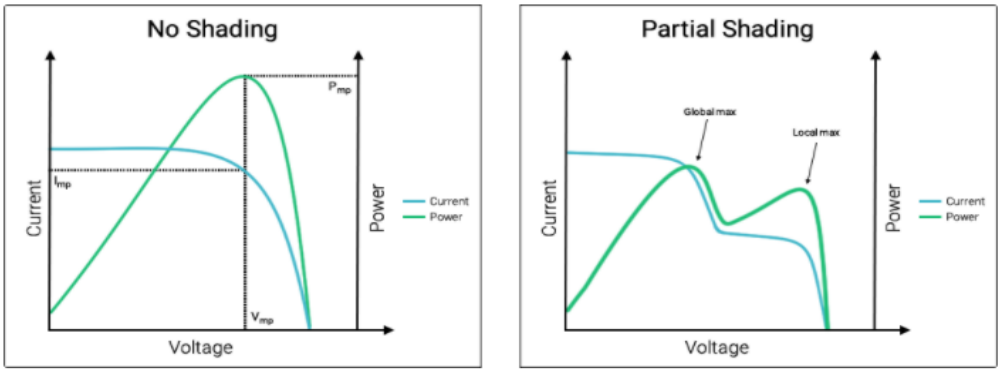

Fig. (3.14). (left) I-V (blue) and P-V (green) curve of a solar array with no shading; (right) I-V (blue) and P-V (green) curve of a solar array with shading.

3.9 THE IV RECTANGLE

Calculate the power (P) in the circuit which is ideally multiplying the current in phase, I_{sc} times V_{oc}. And when you increase the voltage in the cell. Therefore, the curve rapidly decreases beyond a specified point and consequently there is a constant rise in power with increasing voltage, before we fall off the "cliff" of the curve. There is a point where we will get the maximum power which is the point known as the maximum power point or (MPP) as shown in figure(3.15) [47] . When doubling the current by voltage at the maximum power point is the same thing as calculating the area of a rectangle on the curve. This rectangle will always be less than the required maximum. If there is a method for obtaining the power = I_{sc} * V_{oc}, then it can be calculated as a result of considering area calculations. Scientists define a term called fill factor (written as **FF**), which describes how much energy we get from the cell compared to I_{sc} * V_{oc} .

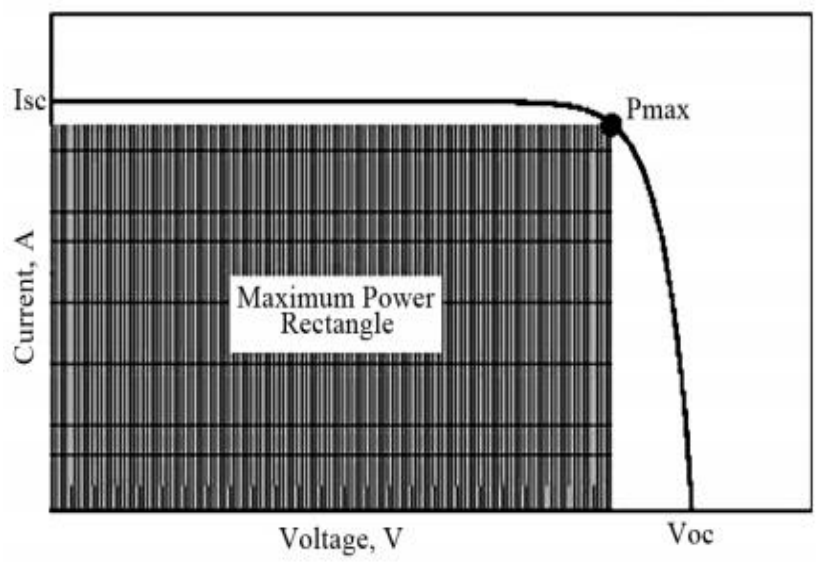

Fig (3.15). The IV And Power Curves For a solar Cell

In other words, the fill factor is how close we are to "filling" the Isc x Voc rectangle.

From the aforementioned we explain that the current often depends on the area of the solar cell in question in order to compare the currents more equitably. The current density is usually used, which is the current divided by the area (usually in units of milliamps per cm^2).

So it is often you see this symbol instead of the current I that we've talked about so far, as we see in the Fill Factor (ff) model equation below.

$$ff = \frac{P_{max}}{V_{oc}} = \frac{I_m V_m}{I_{sc} V_{oc}} \tag{3.13}$$

3.10 CALCULATE OF SOLAR CELL EFFICIENCY

Calculating efficiency is one of the most important measurements at the end of the day, because it determines how much electricity you can get from solar cells. It is defined as the ratio of the energy a cell exits to the energy it enters with sunlight. We can calculate it by noting that the input force is the ideal (I_{sc} * V_{oc}) multiplied by the fill factor (ff). If we know the input energy density (or radiation) of the sun , then divide the two[37,47]:

$$P_{max} = I_{sc}V_{oc}ff \tag{3.14}$$

$$\eta = \frac{I_{sc}V_{oc}ff}{E*A_c} \tag{3.15}$$

$$\eta = \frac{P_{max}}{E*A_c} \tag{3.16}$$

Where:

P_{max} is the maximum power output.

E is the incident flux.

A_c is the area of collector.

V_{oc} is the open-circuit voltage.

I_{sc} is the short-circuit current.

ff Is the fill factor.

η is the efficiency.

3.11 MAXIMUM POWER POINT TRACKING (MPPT) .

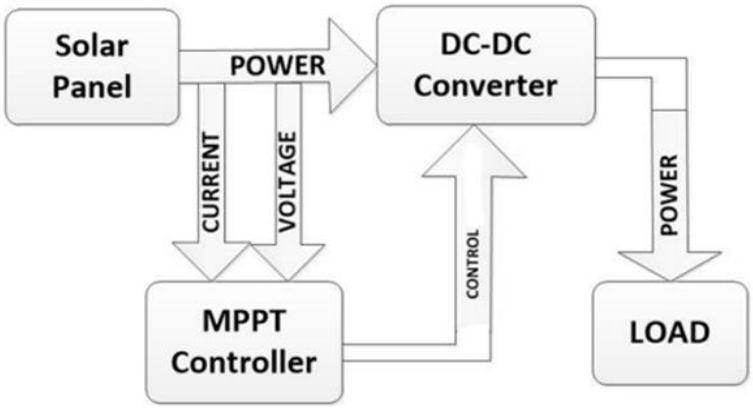

Fig(3.16). Basic Block Diagram Of MPPT In PV System

From the shown in figure (3.16). MPPT algorithms are essential in photovoltaic applications because the MPP of the solar panel varies with different irradiance and temperature and The

maximum power is generated by the solar module at the point (I-V) where the output voltage and current is [Power (W) = Volts (V) * Amps (A)]. This point is known as MPP.

The role of MPPT is to ensure that the PV module runs on its MPP, extracting the maximum amount of available power. If we get good irradiance and proper temperature, the photovoltaic system can generate maximum energy efficiently while using the efficient MPPT algorithm with the system [48-52].

3.11.1 Different MPPT Techniques

There are Different techniques used to track the maximum energy point. Among all the algorithms, P&O and Inc algorithms are the most popular as they have the advantage of easy implementation. Under normal conditions, the PV curve only has one maximum point, so it is not a problem. However, if the PV matrix is partially shaded, there are several extremes in these curves. Among the most common techniques are [49]:

1. Perturbation and Observation (P&O) method.
2. Incremental Conductance (INC) method.
3. Fractional short circuit current method.
4. Fractional open circuit voltage method.
5. Neural networks.
6. Fuzzy logic.

3.11.2 Perturbation and Observation (P&O) Method

The advantage of this method is that it is simple, easy to implement, and the algorithm most commonly used. , P&O is based on the variation of the output voltage of the PV module, and comparing the energy currently supplied by the solar cells with the energy obtained at the previous moment in time and therefore this method was chosen [48].

The P&O algorithm works by continuously measuring the terminal voltage and current of the PV array, continuously disturbing the voltage by adding a small perturbation, and then monitoring changes in the output power to determine the next control signal as shown in figure (3.17).

If the output power increases, the turbulence will continue in the same direction in the next step, otherwise the turbulence direction will be reversed.

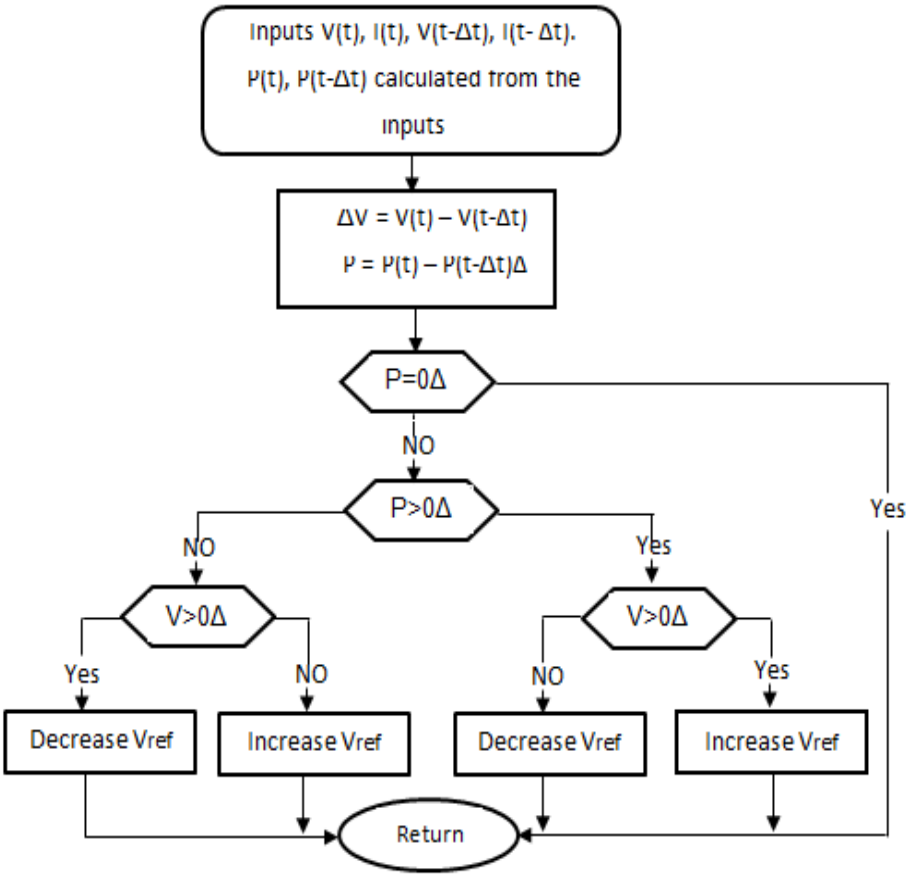

Fig (3.17). State flowchart Of P&O MPPT Technique.

To improve tracking speed and algorithm accuracy, perturbation must be constantly adjusted. By observing the characteristic curves of the photovoltaic cells [49, 53].

By observing the characteristic curves of PV cells, the power increment dP and voltage increment dV satisfy .

At the left of MPP: **dP / dV > 0**

At the right of MPP: **dP / dV < 0**

At the MPP: **dP / dV =0**

That is, when the operating point of the PV module is to the left of the photovoltaic curve (dP positive), which means the output power of the PV module increases, and then the voltage perturbation of the PV module will continue in the same direction towards MPP.

If the unit operating point is on the right side of the P-V curve, the controller will move the PV module operating point backwards in search of true MPP. This can be accomplished by reversing the direction of the perturbation. The diagram for this method is shown in Figure (3.18) [54-57].

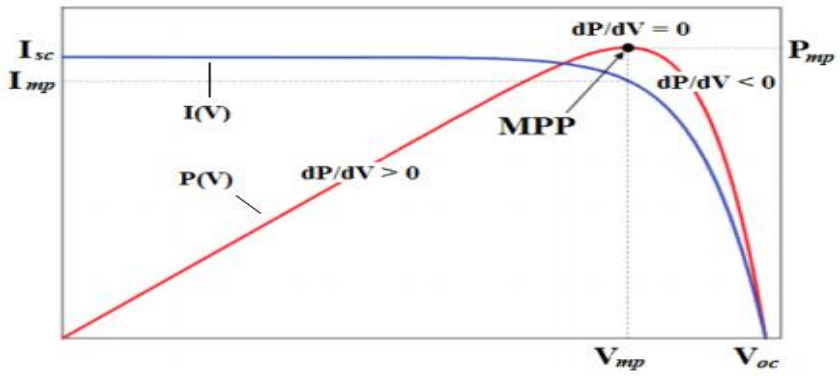

Fig (3.18). a Perturbation and Observation Method Technique Block Diagram Of PVS

3.12 DC-DC CONVERTER

A DC-to-DC converter is a device that accepts a DC input voltage and produces a DC output voltage. In addition, DC-to-DC converters are used to provide noise isolation, power bus regulation[58]. The selection from the variety of available topologies is based on such considerations such as cost, performance and control characteristics, which are determined by the application requirements. No topology is better or worse than the other. Each topology has advantages as well as disadvantages and so the choice is a question of the needs of the user and the system application [59] .

3.12.1 Types of DC-DC Converter

The DC-DC converter is defined as an electrical circuit and its function is to convert DC voltage From one value to another value, up or down, depending on the availability of supply and the requirements of the load, that is, it raises the voltage level up or down. The variable DC voltage level can be regulated by controlling the operating ratio (on-off time of the switch) of the transformer [53,60, 61].

There are different types of DC transformers that can be used to transform the voltage level. We mention some of them .

1. Buck converter.
2. Boost converter.
3. Buck-Boost converter.

1. Boost Converter Design

The boost DC converter is used to step up the input voltage by storing energy in an inductor for a certain time period, and then uses this energy to boost the input voltage to a higher value. The circuit diagram for a boost converter is shown in figure (3.19)

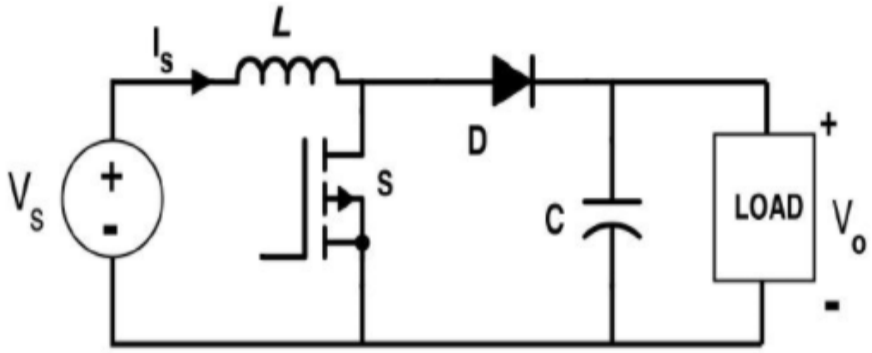

Fig(3.19). Boost Converter

When switch Q is closed, the input source charges up the inductor while diode D is reverse biased to provide isolation between the input and the output of the converter. When the switch is opened, energy stored in the inductor and the power supply is transferred to the load. The relationship between the input and output voltages is given by[41].

$$V_{in}t_{on} + (V_{in} - V_{out})t_{off} = 0 \qquad (3.17)$$

$$\frac{V_{out}}{V_{in}} = \frac{t_{on}+t_{off}}{t_{off}} = \frac{1}{1-d} \qquad (3.18)$$

3.13 ULTRA-CAPACITOR (UC) MODEL

Ultra-capacitor (UC), also known as super-capacitor, is a popular energy storage device for many applications because of its power density and ability to store and release power within short time periods [53].

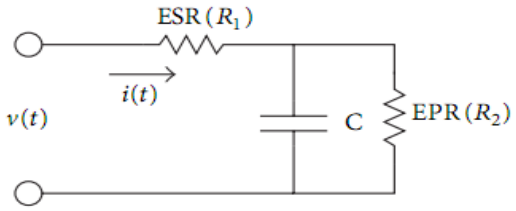

Fig(3.20). Equivalent Circuit For Ultra-Capacitor

Figure (3.20) shows the classical model for ultra-capacitor (UC) used as energy storage device in this work mainly to provide the system by electrical energy when solar irradiance below 1000W/m2 and hence the power produced by PV system should be constant for different weather condition during the day. The model consists of an ideal capacitor, equivalent series resistance ESR and equivalent parallel resistance EPR.

1. **ESR** (Equivalent Series Resistance) is small and simulates heat losses and charge/discharge voltage transient mutation in charging/discharging process.

2. **EPR** (Equivalent Parallel Resistance) is a large resistance representing the current leakage effect and impacts long-term energy storage with capacitor initial voltage charging of 300 volt .

3.13.1 Bi-Directional dc-dc Converter

The bidirectional dc-dc converter along with energy storage has become a promising option for many power related systems, including hybrid vehicle [53] fuel cell vehicle, renewable energy system and so forth. It not only reduces the cost and improves efficiency, but also improves the performance of the system. In renewable-energy applications, the multiple-input bidirectional dc-dc converter can be used to combine different types of energy sources. In photovoltaic system applications, an auxiliary energy storage like an ultra-capacitor is been used. With its ability to reverse the direction of the current flow, and thereby power, the bidirectional dc-dc converters are being increasingly used to achieve power transfer between two dc power sources in either direction. Most of the existing bidirectional dc-dc converters fall into the generic circuit structure which is characterized by a current fed or voltage fed on one side [53]. Based on the placement of the auxiliary energy storage, the bidirectional dc-dc converter can be categorized into buck and boost type. The buck type is to have energy storage placed on the high-voltage side, and the boost type is to have it placed on the low-voltage side. Figure (3.21) represents the implementation of a bid- irectional DC/DC converter with ultra-capacitor storage device.

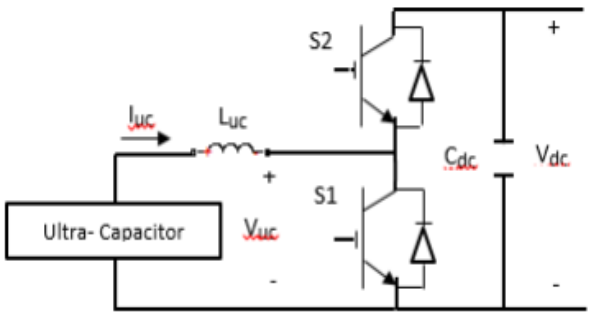

Fig(3.21) Implementation Of a bi-Directional DC/DC Converter

3.14 DC – AC INVERTERS

The voltage inverters (DC-AC) is used to convert the direct current (DC), from the solar cells to the frequency (AC) to feed it the loads, so choose the voltage converter that fits the system, because of the primary role it plays. When designing a complete PV inverter, one must choose

between single phase and three phase inverters. Single phase inverters are often favoured by power ratings below circa 5-6 kW, and subsequently three-phase above this rating [54,62].
Based on their operation the inverters can be broadly classified into:

1) Voltage Source Inverter (**VSI**).
2) Current Source Inverter (**CSI**).

1. Voltage Source Inverter (VSI).

A voltage source inverter is supplied by a DC voltage source, the DC source is usually an AC/DC rectifier. There is a large capacitor used to keep the DC-link voltage stable. Usually, a VSI has buck operation function. Its output voltage peak value is lower than the DC link voltage. It is necessary to avoid a short circuit across the DC voltage source during the operation. If a VSI operates in bipolar mode, that is, the upper switch and lower switch in a leg work to provide a PWM output waveform, the control circuit and interface have to be designed to leave small gaps between switching signals to the upper switch and lower switch in the same leg. [63,64].

2. Current Source Inverter (CSI).

A current source inverter is supplied by a DC current source. the DC current source is usually an AC/DC rectifier with a large inductor to keep the supplying current stable. Usually. Its output voltage peak value is higher than the DC link voltage.
Since the source is a DC current source, it is necessary to avoid open circuit of the inverter during operation. The control circuit and interface have to be designed for small overlaps between switching signals to the upper switches and lower switches at least in one leg. [64].

3.15 SIZING OF PV GRID CONNECTED SYSTEM PROCEDURE

Sizing PV grid-connected system is a relatively simple procedure compared with standalone system because the system is connected to the national grid. So if the PV array produces more energy than the loads need, the extra energy can be delivered to utility grid, in the case of PV array cannot meet the loads demand, utility grid will provide electricity for the loads[65-67].
Therefore battery bank is not necessary for grid connected systems. The sizing of PV grid-connected system involves site weather conditions, loads analysis, module and inverter selection. The PV system proposed in this thesis is to fed certain ratio of the total energy consumption in the clinic and planned to cover essential loads represents in emergency site and other some important loads during daylight period.

3.15.1 PV Array Sizing

Photovoltaic (PV) modules are sized using wattage determined under Standard Test Conditions (STC). This is the manufacturer's specified nameplate wattage and represents in module output measured under very controlled factory conditions. Specifically, STC are 1000 W/m^2 (solar irradiance) and 25^oC (module temperature) [58]. The sizing criteria for PV module are based manufacturer's data, system DC voltage and orientation which is represented in optimum tilt angle in the selected site. Three items need to be addressed when sizing a PV array and they are as follows[68].

A) Module Selection

Module selection is based on the specifications provided by the manufacture. Specifications such as performance, physical size and cost must be compared between different modules before the decision on which module(s) to use is made. In this work, mono crystalline solar module has been selected for PV system sizing because of a higher efficiency, more available than poly silicon solar cells and more space-efficient, i.e. they yields highest power output and the least amount of space than the polycrystalline[38].

B) Number of Modules

The number of modules connected in series (this is called a string) determined by dividing the designed system voltage with the nominal module voltage that occurs at lower temperatures. The number of modules in series , N_s, is calculated by:

$$N_s = V_{DC}/V_m \quad (3.19)$$

Where ;

N_s : Number of modules connected in a string.

V_{DC} : The selected DC bus voltage (volt).

V_m : The module voltage for operating conditions.

The number of modules in parallel, N_p, is determined by dividing the designed array output (W_p) by the selected module output (W_p) and the number of string.

$$N_p = E_L / A_{om} \quad (3.20)$$

$$A_{om} = N_s * P_m * t \quad (3.21)$$

Where;

N_p : Number of strings required in parallel.

E_L : Average daily load energy (Wh/d).

A_{om} : Average daily energy generated from the string (kWh).

P_m : Maximum power under standard condition (Watt).

t : Equivalent hours of PV operation (hour).

3.15.2 Selecting the Inverter

An inverter is used in order to change the direct current (DC) generated by the solar panels to alternating current (AC) for the loads. Selection for grid-connected solar PV systems is a very important step because of the role the inverter plays in the whole system as the main connecter to the utility grid. Inverters have to be sized such that to handle the expected power level, and be compatible with the specifications on the grid side. Most inverters now days have at least one Maximum Peak Power Tracking (MPPT) output. The MPPT applies the proper resistance to find the optimal maximum power point. With a MPPT the panel can operate at the optimal working range. Since the power requirements of the inverter is driven by the load demand, the inverter must be chosen so that it can meet the maximum load demand and still remains efficient at the level it will be used the most . The following points should be addressed when choosing an inverter [64,69].

1- The input voltage of the inverter must be rated to handle the full range of the power conditioning. A sensing circuit is useful to prevent damage when operation of the inverter is below or beyond its optimal operation points .

2- The inverter should be rated at least 20% more than the maximum power requirement of the load to ensure that it can deliver this power for an extended time .

3- It may be useful to choose more than one inverter for an application with variable loads in order to have the inverter operating at its maximum efficiency for a range of power requirements. Multiple units connected in parallel to service the same load must be compatible and their frequency must be inter-regulated to be in phase .

4- The output alternating current of the inverter must be sine wave current with a voltage of 380V, 50Hz to facilitate synchronization with the grid.

Since in this design we have 400 module connected to inverter. From table (3.2), the inverter input voltage V_{min} = 200V, V_{max} = 1000V, so when chosen 410V as DC voltage panel output for each string with module voltage of 41 V.

Therefore the number of modules in series = 410/41 = 10 and the number of parallel modules = 400/10 = 40 modules for 10 strings and which is equal to 4 modules for each string.

The output power of a solar module is affected by the temperature of the solar cells.

This variation in power due to temperature is also reflected in a variation in the open circuit voltage and maximum power point voltage.

With the odd exception grid interactive inverters include

- Maximum Power Point (MPP) trackers .
- Many of the inverters available will have a voltage operating window.

When the temperature is at a maximum then the Maximum Power Point (MPP) voltage (V_{mp}) of the array should never fall below the minimum operating voltage of the inverter. It is assumed that maximum effective cell temperature of 70°C is used. The module selected has a rated MPP voltage of 41.0 V and a voltage (Vmp) coefficient of 0.133V/°C. And with the effective cell temperature of 70°C is 45°C above the STC temperature by 25°C .

Therefore the V_{mpp} voltage would be reduced by 45 x 0.133 = 5.985V. The V_{mpp} at 70°C would be (41 - 5.985 = 35.015V). And by Assuming a maximum voltage drop in the cables of 3% then the voltage at the inverter for each module would be (0.97 x 35.015 = 33.965V) .

This is the effective minimum MPP voltage input at the inverter for each module in the array .

The minimum voltage window for an inverter is 315V, with recommended that a safety margin of 10 % is used. Therefore, minimum inverter voltage of 1.1 x 315V = 346.5V should be used .

The minimum number of series modules in a string is = 346.5/33.965 = 10.2 rounded to 10 modules [53].

At the coldest daytime temperature of the open circuit voltage of the array shall never be greater than the maximum allowed input voltage for the inverter.

Therefore the lowest daytime temperature for the area where the system is installed shall be used to determine the maximum V_{oc} .

By considering the minimum effective cell temperature is 15°C, with the open circuit voltage (V_{oc}) of 48.6 V and a voltage (Voc) co-efficient of -0.14V /°C.

An effective cell temperature of 15°C is 10° below the STC temperature of 25°C. Therefore the V_{oc} Voltage would be increased by 10 x 0.14 = 1.4V.

The V_{oc} at 15°C would be 48.6 + 1.4 = 50V.

According to used inverter specifications, the input maximum voltage allowed is 1000V .

The maximum number of modules in series is = 1000 / 50 = 20 modules.

Ten inverters from Technical data technology are selected for system sizing. The nominal AC power of the selected inverter is 10 kW ،3-phase with maximum power point tracker (MPPT) built in and have maximum efficiency of between 98% and 98.3%.

3.16 SYSTEM SPECIFICATIONS

The designed system size and specifications are provided for the 88 kW (tables 3.2) power plant are as follows :

TABLES 3.2: PV Power Plant Specifications At 25^0 C, 1000 w/m^2

Solar photovoltaic power plant specifications at stc	
Plant capacity	88 KW
Voltage output	410 V
Current output	214.8 A
No of modules	400
Available area	650 m2
Solar panel specifications	
Type	mono-crystalline
Rated power	220W
Rated Voltage (Vmpp)	41.0V
Rated Current (Impp)	5.37A
Efficiency	17.7%
Temperature	25 deg c
Module Area	1.244m2
Grid specifications	
Number of phases	3-phases
Voltage rating	380 volts
Frequency	50 Hz
Inverter specifications	
Type – Technical data	RPI-M10A
Input DC Voltage Range	200-1000V
MPPT Voltage Range	415-800V
Nominal DC Voltage	600V
Total Input Current	25 A
DC Disconnection Switch	Yes (Inbuilt)
Rated Output Power	10.5 kVA
Max. Output Current	16 A
Nominal AC Voltage	3 Ph, 400 V
AC Voltage Range	400 V ± 20 % (320~480)
Nominal Frequency	50 Hz
Frequency Range	45 Hz - 55 Hz
Power Factor at Rated Power	Unity
Harmonics	<3% at Rated Power
Maximum Efficiency	98.30 %
Dimension (H/W/D)	445 x 510 x 177 mm
Range	(Full Power -20℃ to + 40℃)

The present technology consists of the string inverters and the ac module. The string inverter is A reduced version of the centralized inverter, where a single string of PV modules is connected to the inverter. The input voltage may be high enough to avoid voltage amplification.

This configuration emerged on the PV market in 1995 with the purpose of improving the drawbacks of central inverters, so this topology of connection is selected for this work with using three operation inverters . The rated power output for each PV module at STC is 220 W and the planed PV power solar plant to cover the target loads by supplying energy during day period with taking in account all system losses and performance ratio is 88 KW as well as shown from PV system software simulation results. Therefore the number of PV modules required to install mentioned PV power plant in the selected area can be calculated as follows :

$$NO._{PV} \text{ modules} = P_{PV} / P_{mpp}. \quad (3.22)$$

$$NO._{PV} = 88000/220 = 400 \quad (3.23)$$

PV module from the above result, the system will consist of 400 modules distributed in 10 strings and connected in series-parallel combination, each string contains 40 modules. Figure (3.22) shows the electrical layout of the overall system.

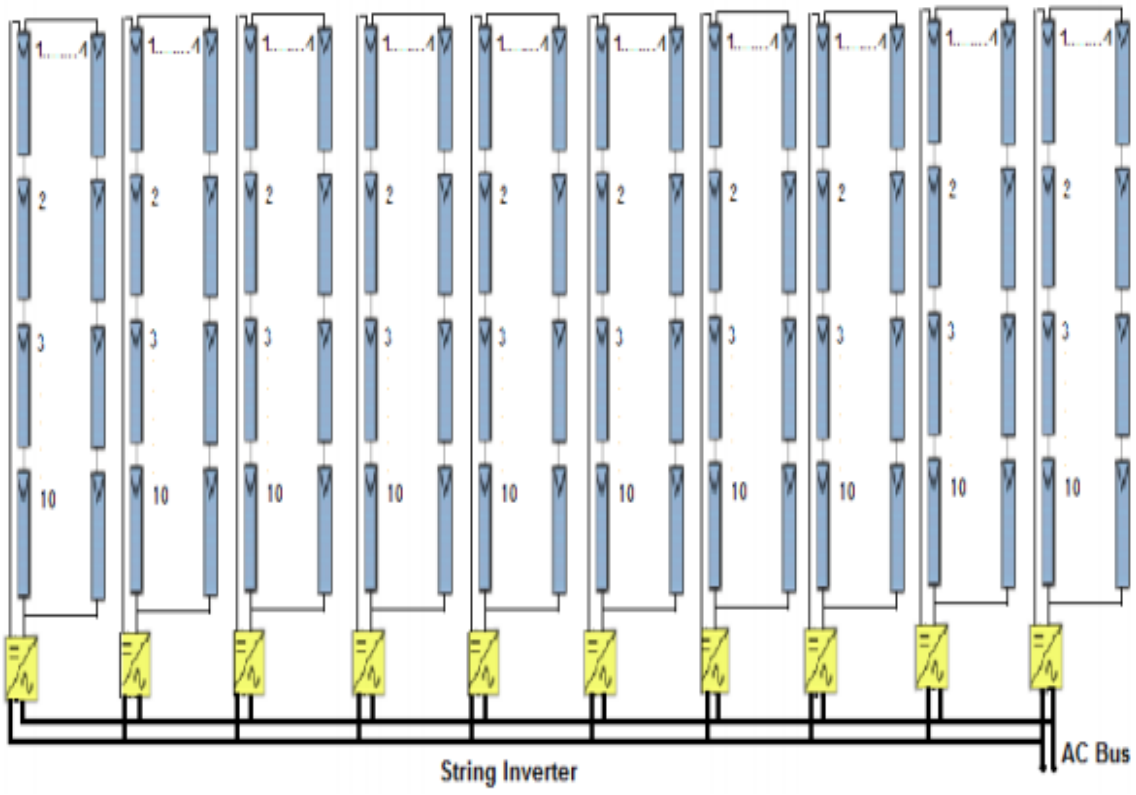

Fig (3.22). PV Grid Connected System Configuration

Compared to central inverters, in this topology the PV strings are connected to separate inverters. If the voltage level before the inverter is too low, a DC-DC converter can be used to boost it. For this topology, each string has its own inverter and therefore the need for string diodes is eliminated leading to total loss reduction of the system .

The configuration allows individual MPPT for each string; hence the reliability of the system is improved due to the fact that the system is no longer dependent on only one inverter compared to the central inverter topology. The mismatch losses are also reduced, but not eliminated .This configuration increases the overall efficiency when compared to the centralized converter, and it will reduce the price, due to possibility for mass production [67, 68].

C H A P T E R FOUR

SIMULATION AND RESULTS

4.1 PV AND WIND GRID-CONNECTED SIMULATIONS

Using MATLAB / Simulink, a hybrid system consisting of a grid-connected wind and solar power systems have been configured. In order to evaluate the performance of the two proposed systems mentioned above and to verify the performance and stability of the model, the three-phase and network-connected system was evaluated in two cases as an indicator of performance.

The first case is the response of the system in normal operation (**steady state operation**) and the second case is variable (**transient operation**) according to a change in the wind speed of turbines and a change in the intensity of radiation on the solar panels.

From the figure (4.1), the general model for the hybrid system connected to the grid shows that the model is identical to the hybrid system and to produce the required power. The maximum wind power in the wind power system is about 60 kW, and the maximum power rating for the solar power system is about 88 kW, which is a total of about 148 kW.

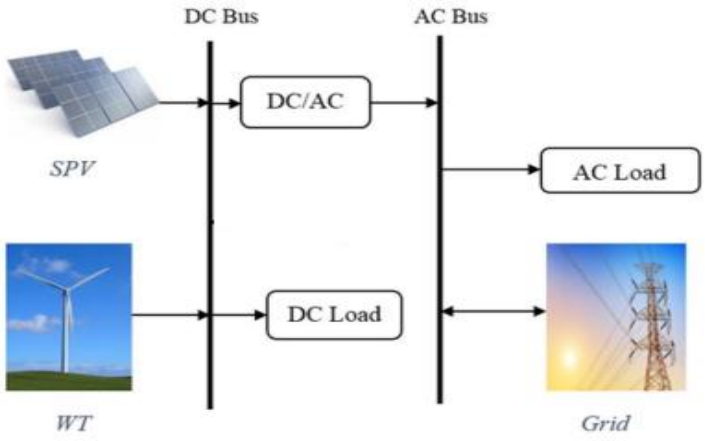

Fig (4.1). Overall simulink model of wind system interfaced with utility

4.2 PV AND WIND SYSTEM DESIGN

The grid-connected system model, which is a hybrid system consisting of solar and wind energy, as shown in Figure (4.2), is designed to supply electrical energy from 10 to 100% of energy demand for all loads associated with the load model in the event of a power outage in national facilities.

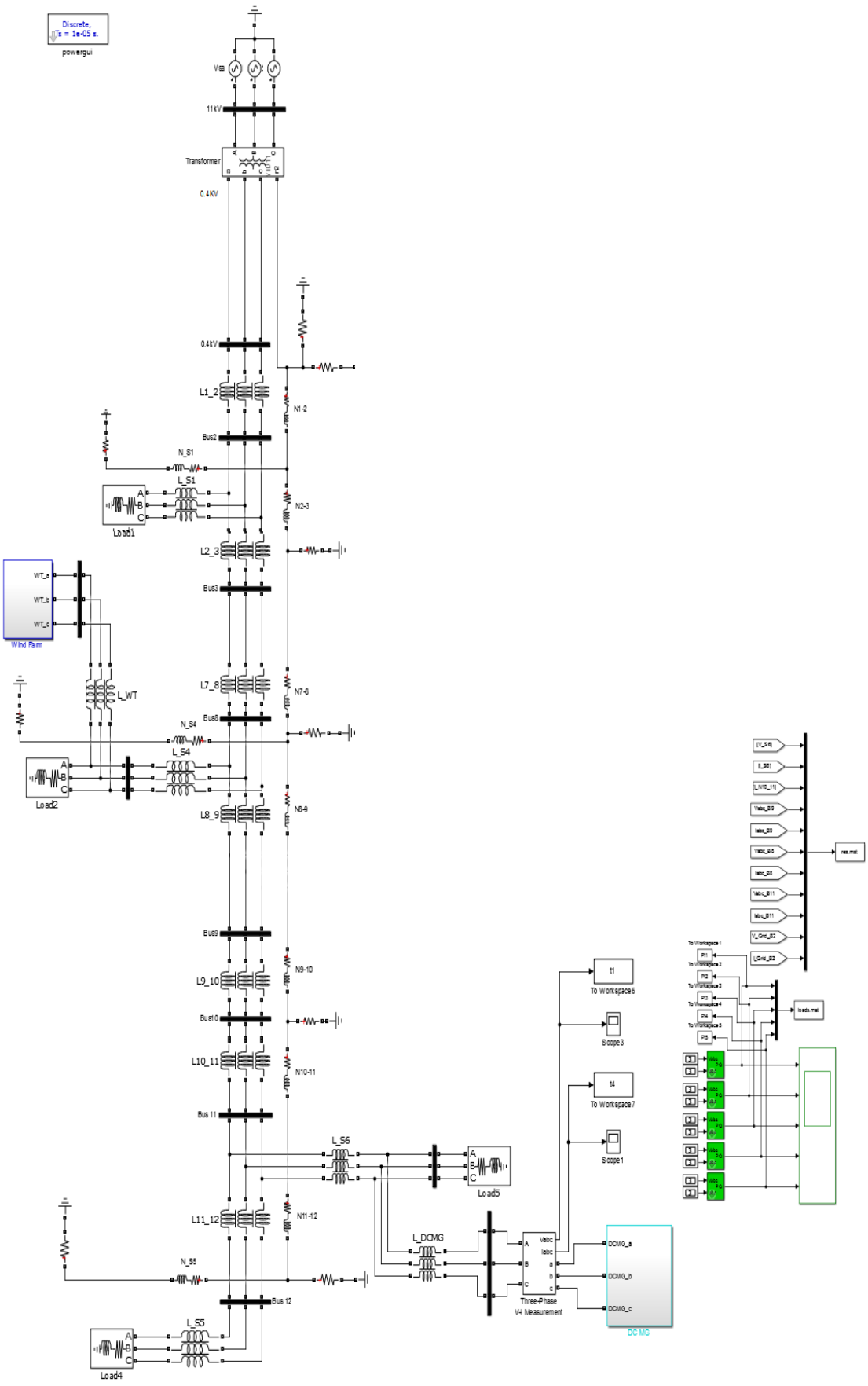

Fig (4.2) Model Wind System Connected Grid

The wind generation potential is determined based on the average annual wind speed according to the location, as well as the generation of solar panels in the availability of the required conditions of radiation intensity and the required temperature, thank God, our country is rich throughout the year. Most modern wind turbines produce energy in the range of 30-40%. Additionally, wind and solar power should be available for a typical day.

The models of a DFIG wind farm shown in figure (4.3) and PV (photo voltage) system shown in figure (4.4).

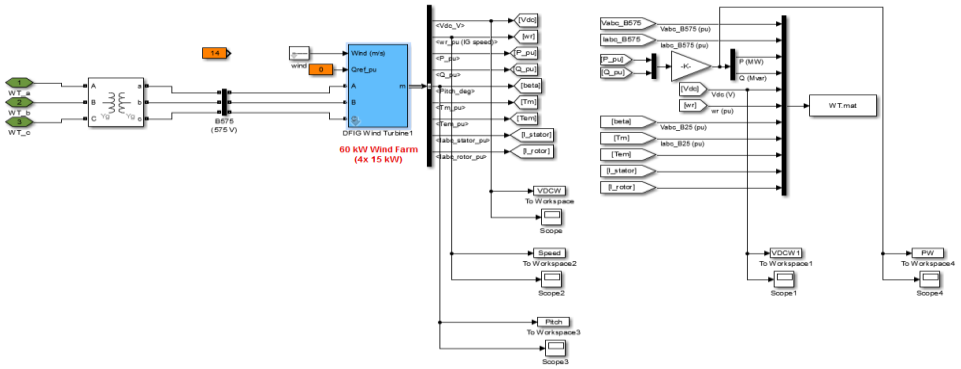

Fig (4.3) Model Of DFIG Wind Farm With a Rating Of About 60 kW

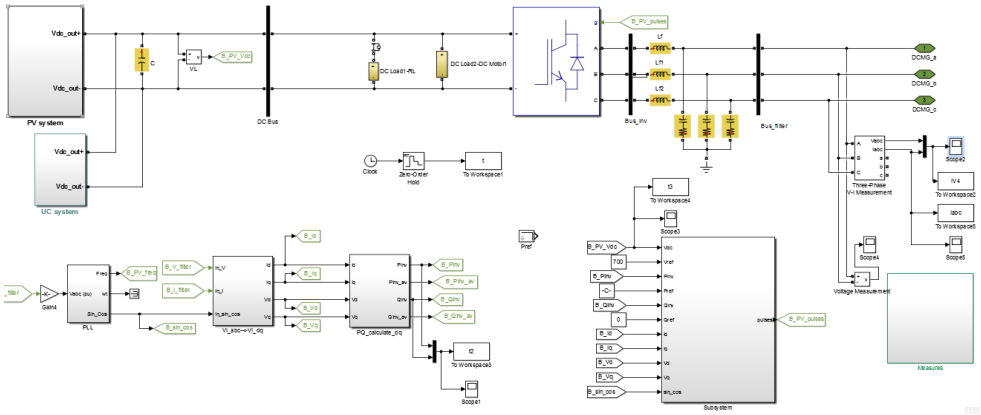

Fig (4.4) Model Of PV System With a Rating Of About 88 Kw

Since Phase Lock Loop (PLL) technique is used for the synchronization between PV system and grid (distribution network) and the inverter topology should guarantee that the output current is a high quality sinewave and in phase with grid voltage .

The resulted voltage and current at point of common coupling (PCC) should be in phase with each other and this can be seen in figure (4.5).

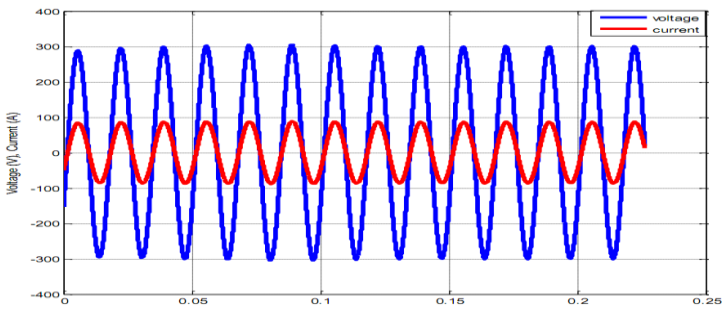

Fig (4.5). Voltage and Current at PCC during Normal Operation

Figure (4.6) shows a three-phase voltage induced by a 3Ø real sine wave inverter after the winding process. The size of the inverter output voltage can be adjusted by adjusting the modulation indicator to match the network voltage.

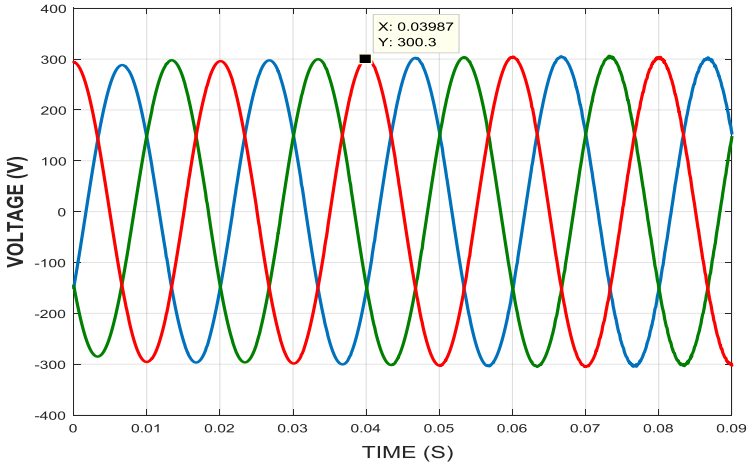

Fig (4.6). Three Phase Voltage Inverter Output

4.3 CASE STUDIES

To evaluate the performance of the modeling and simulation program of the wind and solar system to verify the desired results of the proposed model. Two tests were performed in a networked system and were found to be associated with several performance indicators:

1- System response under normal operation .

2- Change in wind speed, solar radiation**.**

4.3.1 CASE A: STEADY STATE OPERATION

It is through this thesis a preliminary stability study was conducted. During steady state, the distributed generating units operate at their nominal point, providing power to the loads and the grid. The photovoltaic system supplies power to the loads and the grid, and the super-capacitive energy storage system is inactive, that is, neither charging nor discharging. It is evident that the distributed generating units reach steady operating state after a short period of time.

4.3.1.1 Steady State Operation of Wind Turbine System

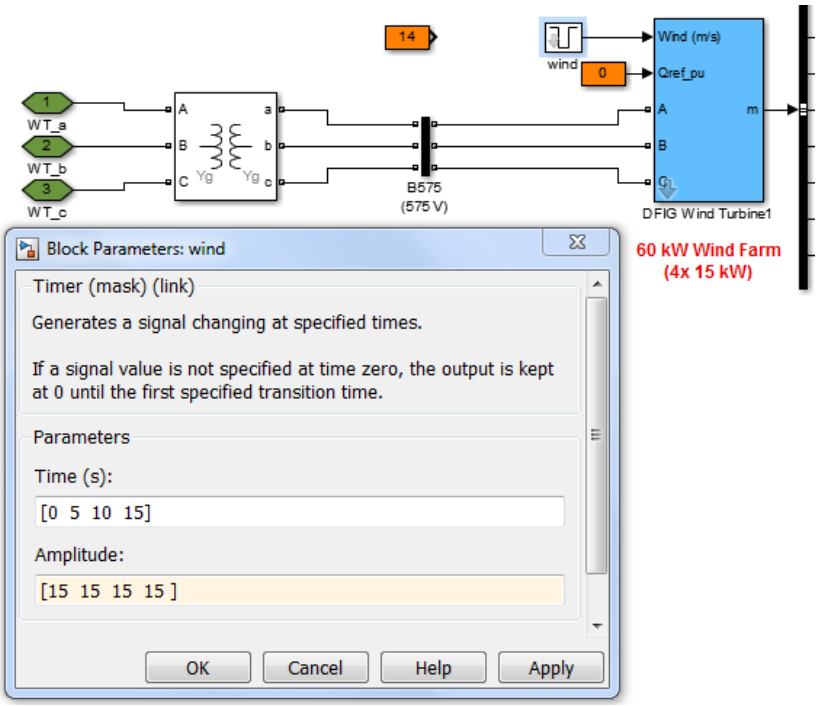

Fig (4.7). Block Parameters Wind Turbine At Stady Stat

At steady state figure (4.7), the distributed generation unit is operating at it is nominal point, and supply power to the loads. Figure (4.8) shows voltage simulation result at DC Link when the system operates at average normal wind speed by magnitude of 15 m/s at time between 0s to 10s

at the beginning of the operating condition the voltage is unstable which known transient situation after that the voltage is stable at 1000 volt DC.

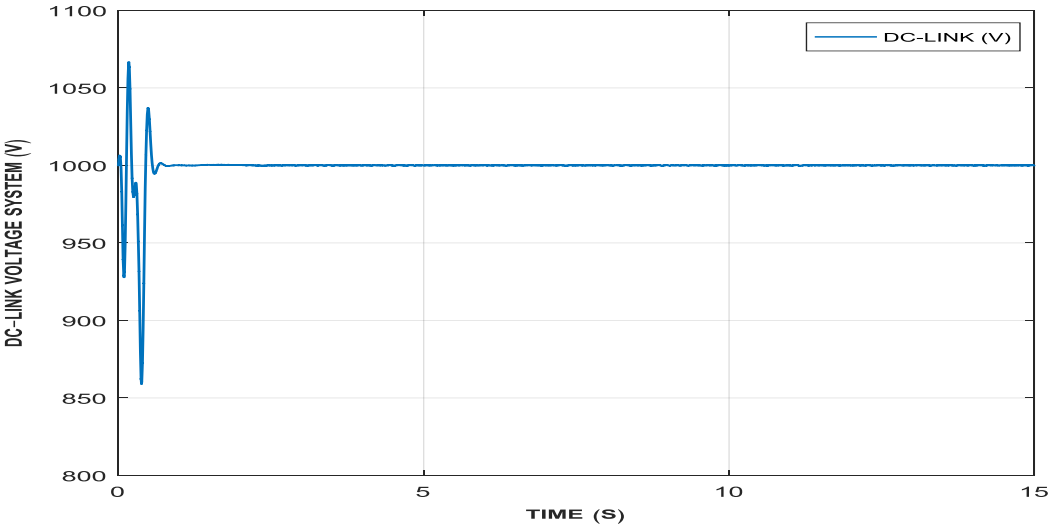

Fig (4.8). DC Link Voltage Wind Turbine System (Vdc steady state = 1000 volts)

In figures (4.9), (4.10). after short period of time in the beginning of the operation, the pitch angle controller was stable, as a result, the pitch angle set at 6.528 deg, therefore the rotor speed was stable Almost at 1.177 pu.

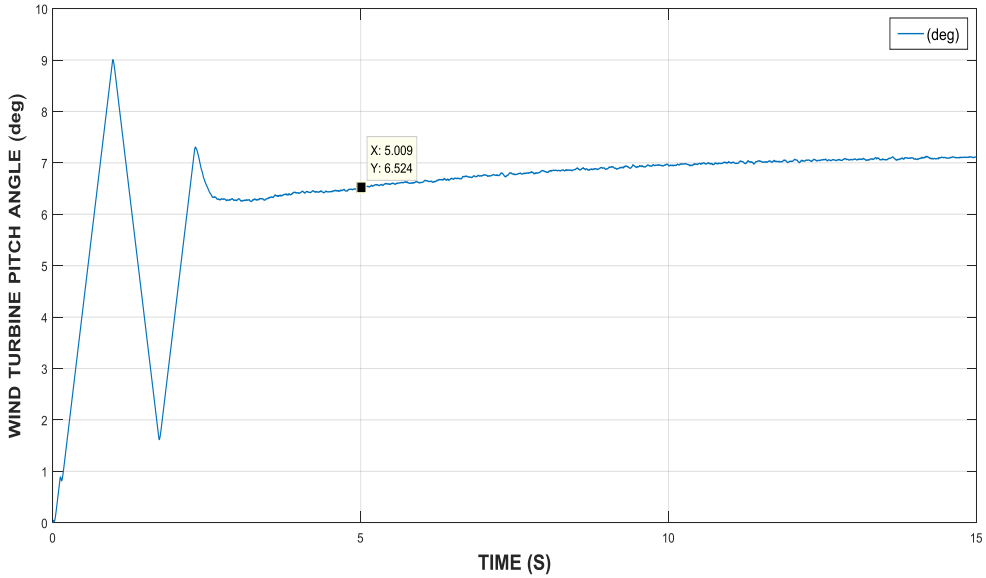

Fig (4.9). Wind Turbine Pitch Angle (deg)

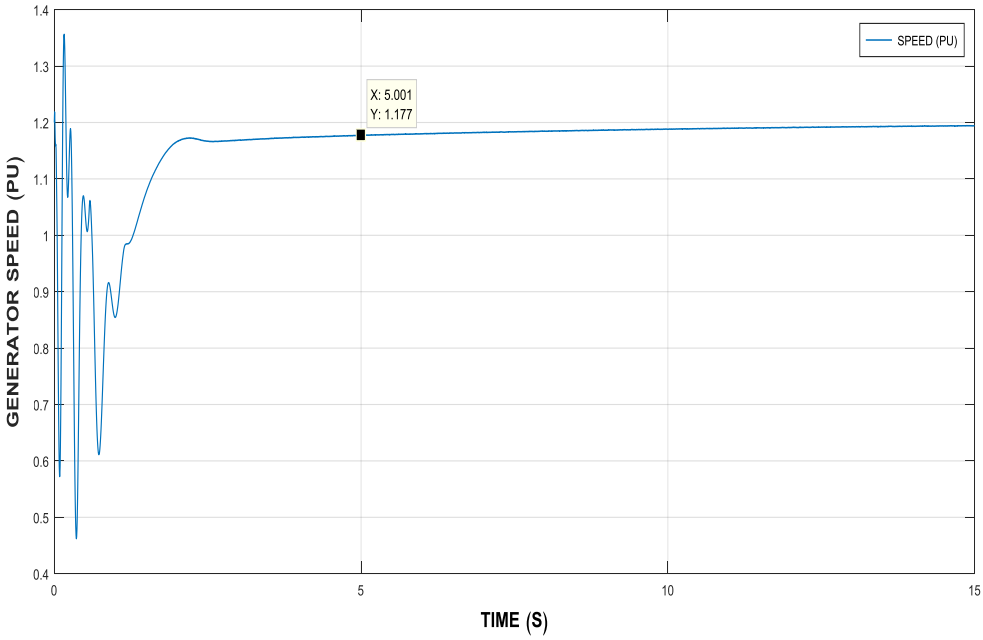

Fig (4.10). Generator Speed (pu)

In figure (4.11), the AC active and reactive power injected into the grid side at point of common coupling. From the figure it is observed that the AC power reaches its nominal value after short period of time and then remain stable at constant value at the steady state operation.

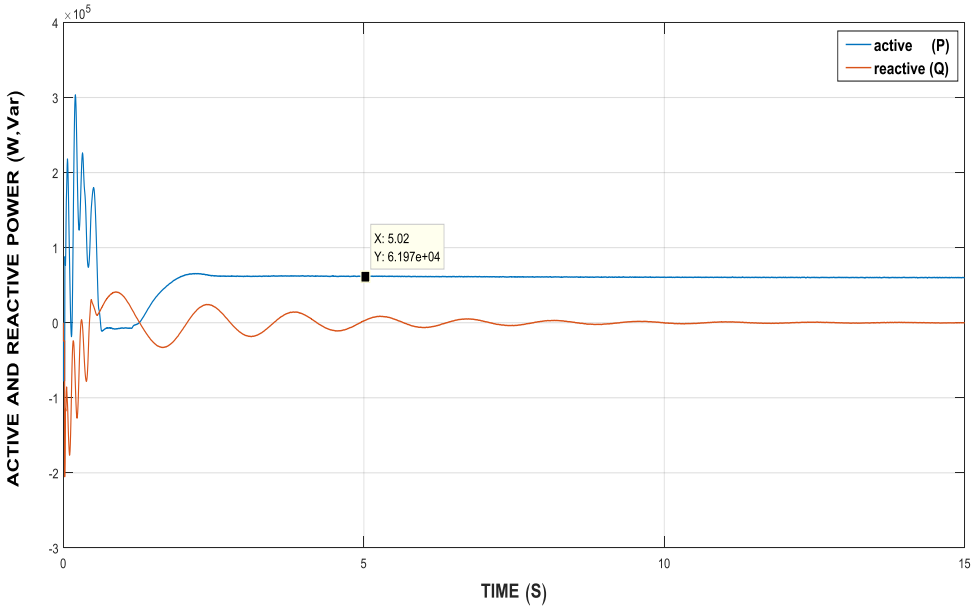

Fig (4.11). Active And Reactive Power Generated By Wind System To The Utility Side (W,Var).

From the figure (4.12) it's observed that the active and reactive power of the loads reach their nominal values after short period of the time and then kept stable at constant values in case of steady state operation .

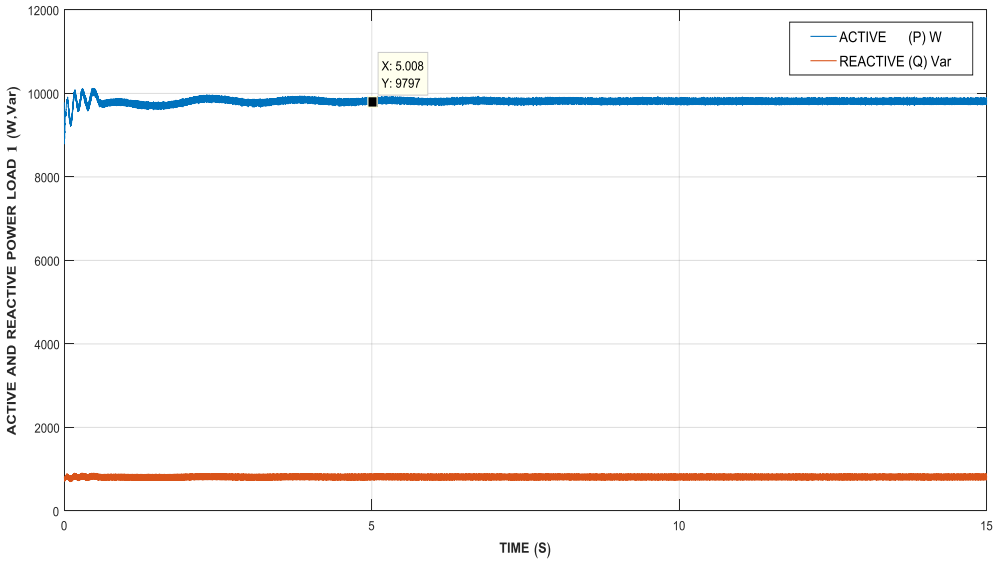

(a) Load 1

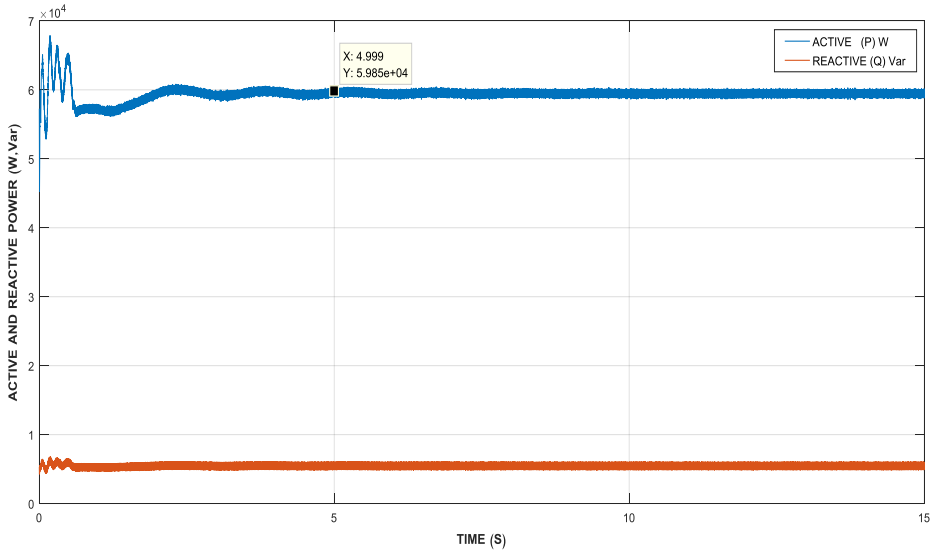

(b) Load 2

Fig (4.12) Active and Reactive Power (W, Var) (a) Load 1, (b) Load 2

4.3.1.2 Steady State Operation of Photovoltage System

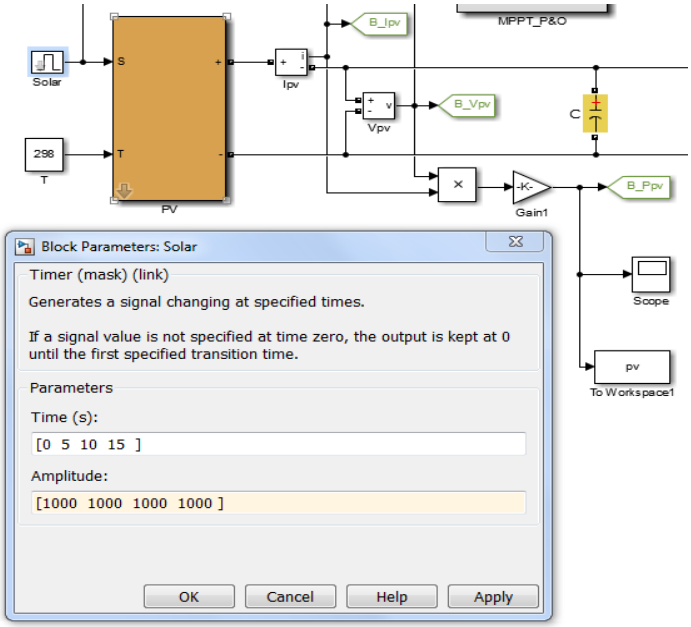

Fig (4.13). Block Parameters Sole Plant At Stady Stat

In a steady state figure (4.13), the system operates at the nominal capacity to supply the loads. Therefore, there is no charge or discharge to the capacitor. Figure (4.14) shows the result of simulating the constant voltage of the system at the voltage distributor under standard operating conditions at 410 V.

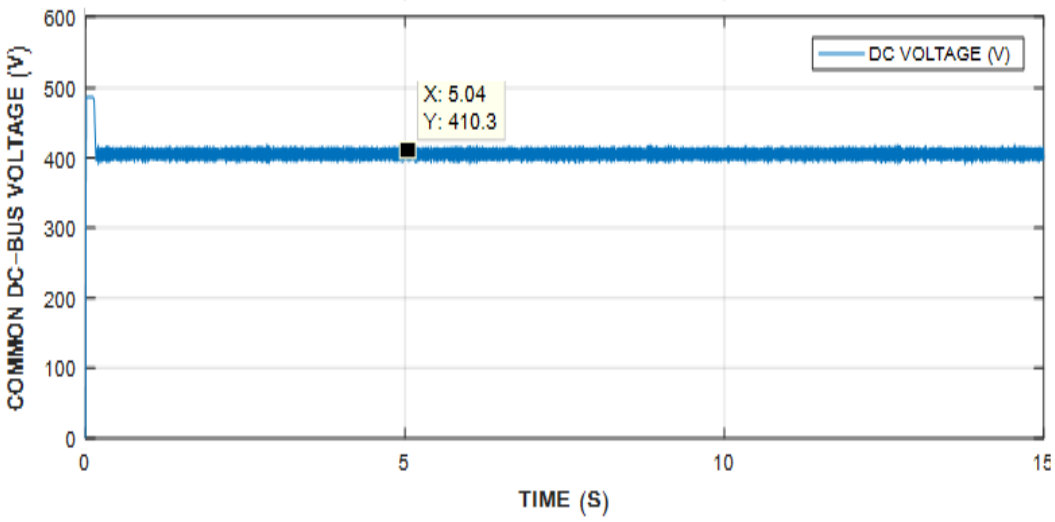

Fig (4.14). Constant Voltage At Stable Voltage Distributor

Since the capacitor was used as an energy storage element in the system to carry out the charging and discharging operations, meaning that the charging process takes place when the radiation rate exceeds 1000 watts / m2 and the discharge process is done when the opposite is done, which

results in the generation of constant electrical power during daylight hours, and the capacitor also has a role in stabilizing System work. Figure (4.15) shows the continuous power produced by the system at steady state.

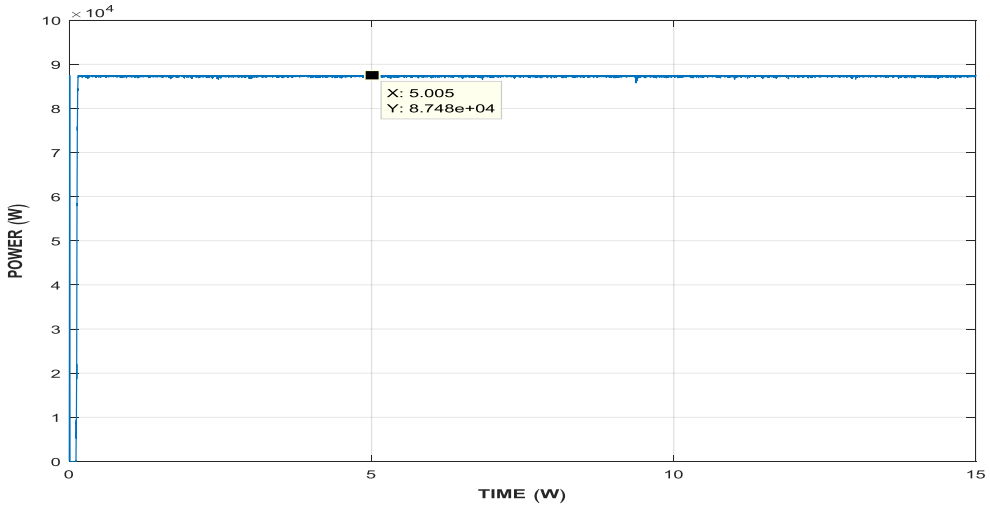

Fig (4.15). The Persistent Power Resulting By The Solar System

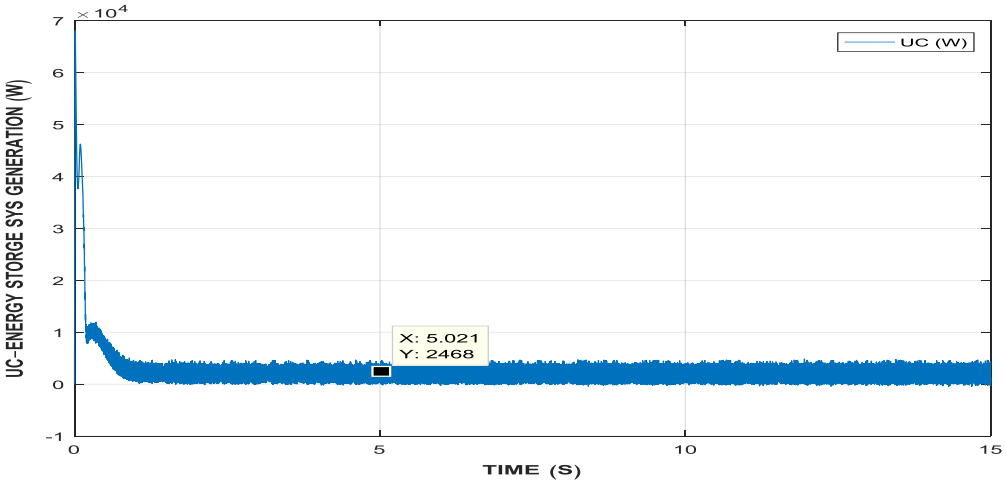

Fig (4.16). UC Energy Storage System Generation

From the previous result, it is noticed that the system acquires its nominal or design capacity when it is commissioned after a short period of time. Figure (4.16) shows the alternating capacity produced by the system to feed the loads, where from the figures (4.17) (4.18) (4.19) we note that the system provides all loads with stable and reliable capacity without any interruption. Or wiggle. There are two types of DC loads included

a) DC resistance as show figure (4.18).

b) DC motor as show figure (4.19).

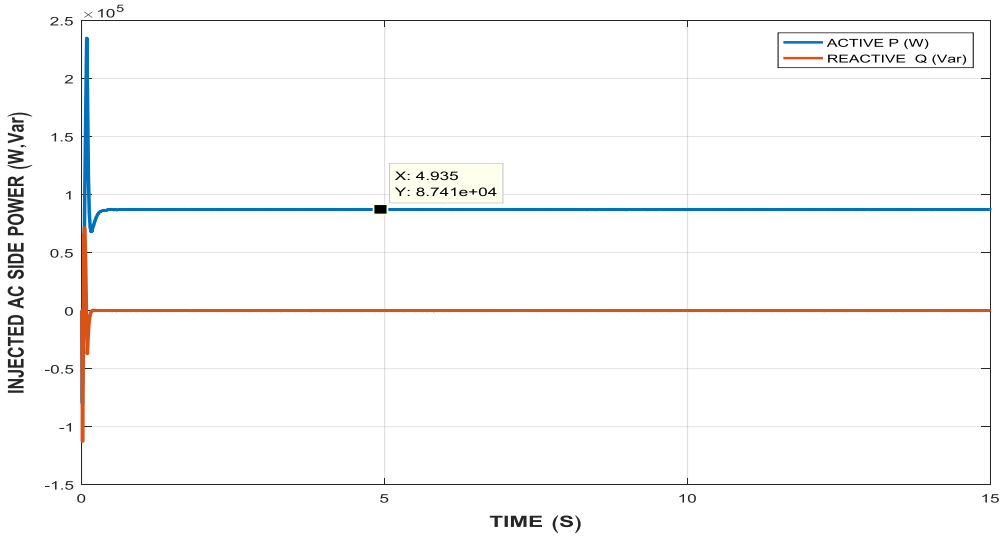

Fig (4.17). Power Injected Into The Utility Grid

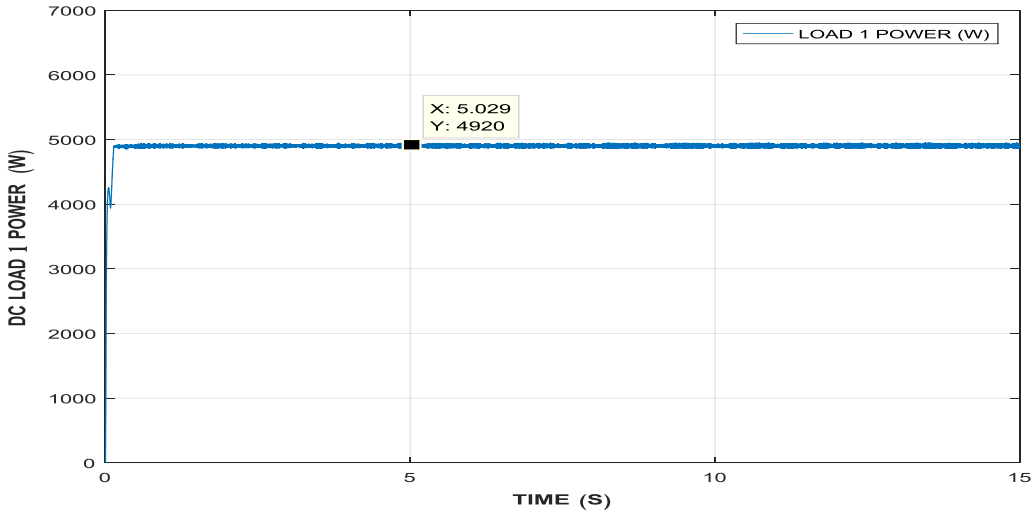

Fig (4.18). DC Load 1 Power(w)

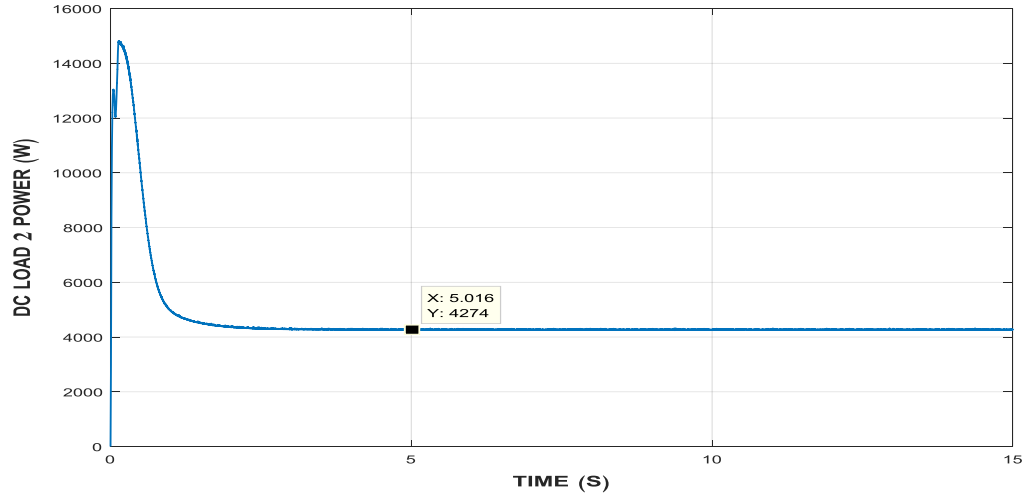

Fig (4.19). DC Load 2 Power(w)

4.3.2 CASE B: TRANSIENT OPERATION

This scenario is to test the system when wind speed fluctuation and changes in solar irradiance occurs**.**

4.3.2.1 Change in Wind Speed of the Turbine System

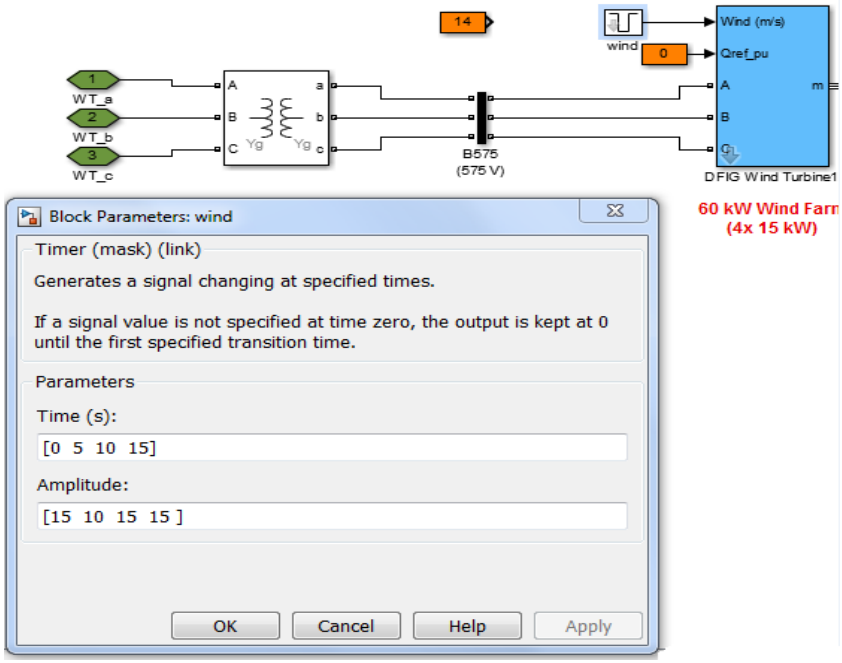

Fig (4.20). Block Parameters Wind Turbine At Transient

When the case is in transient as shown in figure (4.20). Then Simulation result in Figure (4.21), At t=10s, the wind speed increased from 10 to15 m/s, so the DC voltage was constant at its nominal value (1000V_{dc}). Hence, the DC voltages are stable at 1000 Vdc.

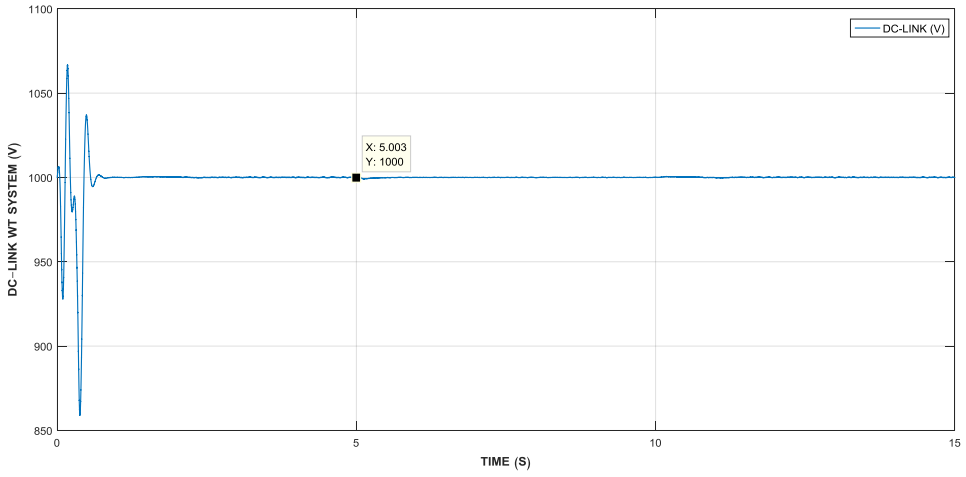

Fig (4.21). DC-Link Voltage WT System (V_{dc})

Simulation results in Figures (4.22), (4.23) and (4.24) noticed that at the beginning of the runtime, a transient condition occurred, and after that, the pitch angle controller regulated the pitch angle at 1.6 °, thus, the generated wind power system was about 215 kW and was the size of the rotor speed is 1 pu.

At the time from t = 5 s to t = 10 s, the wind speed increased from 10 to 15 m / s and stabilized at a speed of 15 m/s, the control unit in the pitch angle regulated the angle of the pitch to 6.5 degrees with the stability of the wind energy generated 60 kilowatts and speed Rotor to 1.175 pu. , So the DC voltage was constant at its nominal value (1000Vdc). Hence, the DC voltages are stable at 1000 Vdc.

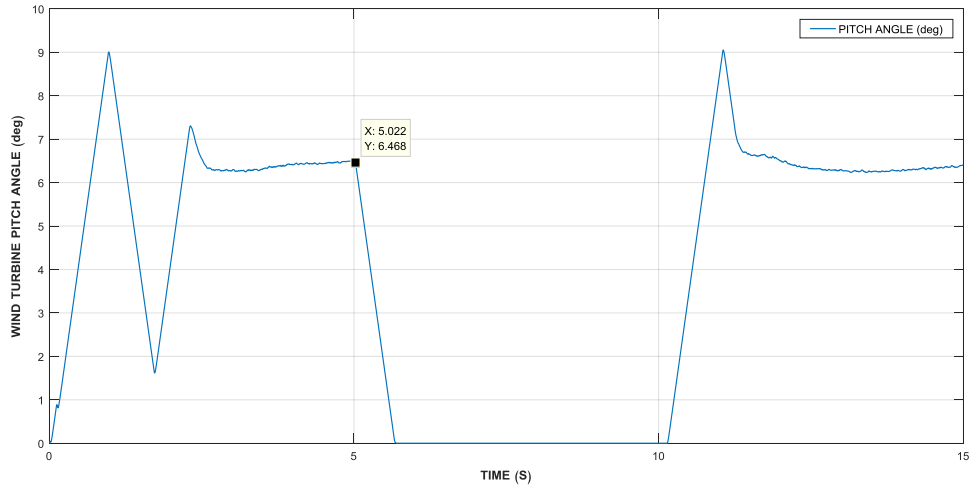

Fig (4.22). Wind Turbine Pitch Angle (deg)

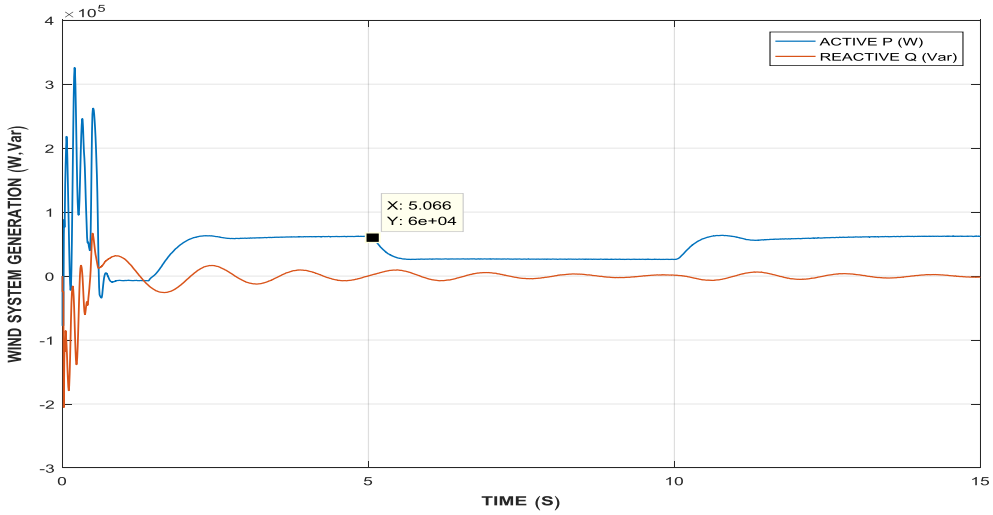

Fig (4.23). Active (w) And Reactive (var) Power

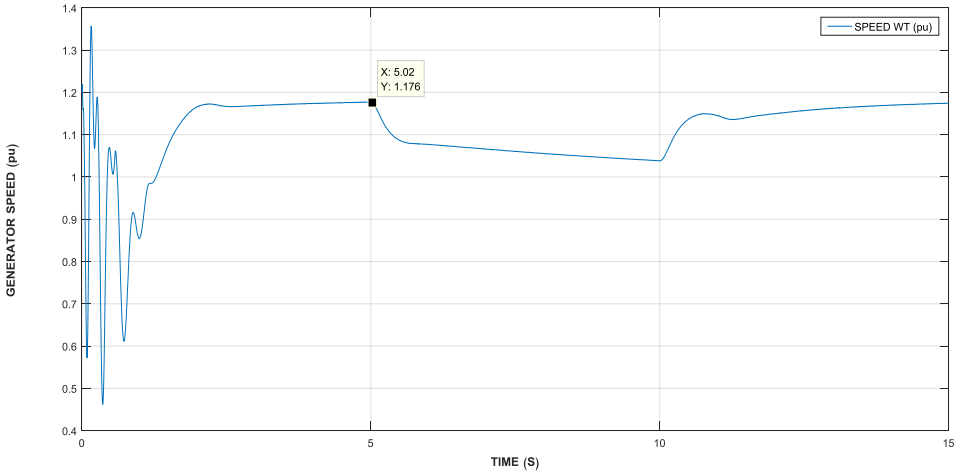

Fig (4.24). Generation Speed (pu)

4.3.2.2 Change in Irradiance of Photovoltage System

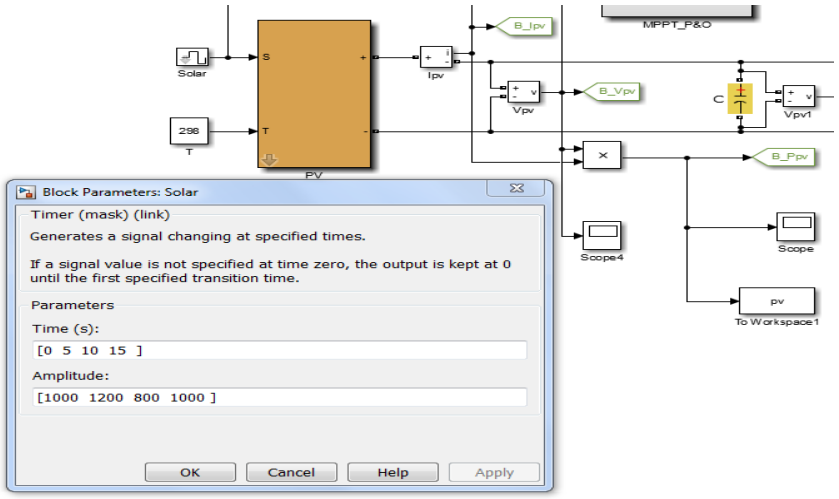

Fig (4.25). Block Parameters Sole Plant At Transient

At transient figure (4.25). From the Figure (4.26) show the continuous power produced by the system as the resulting power increases during the period from (t=5-10 seconds) where the solar irradiance changes from 1000 W/m^2 to 1200 W/m^2 At t=5s, and then at t=10s it changes again from 1200 W/m^2 to 800 W/m^2, and at t=10s it changes again from 800 W/m^2 to 1000 W/m^2 During this period cell temperature is constant at 298 K. Figures (4.27) (4.28) demonstrated the simulation results of the PV system. PV power generation increases with solar irradiance during the period t=5s-10s and the UC energy storage system is charged using the extra power. PV output generation decreases with solar irradiance during the period t=10s -15s and UC is

discharged to provide power for loads. During this period DC and AC loads are unaffected by the PV power fluctuations because of the using UC energy storage in the system.

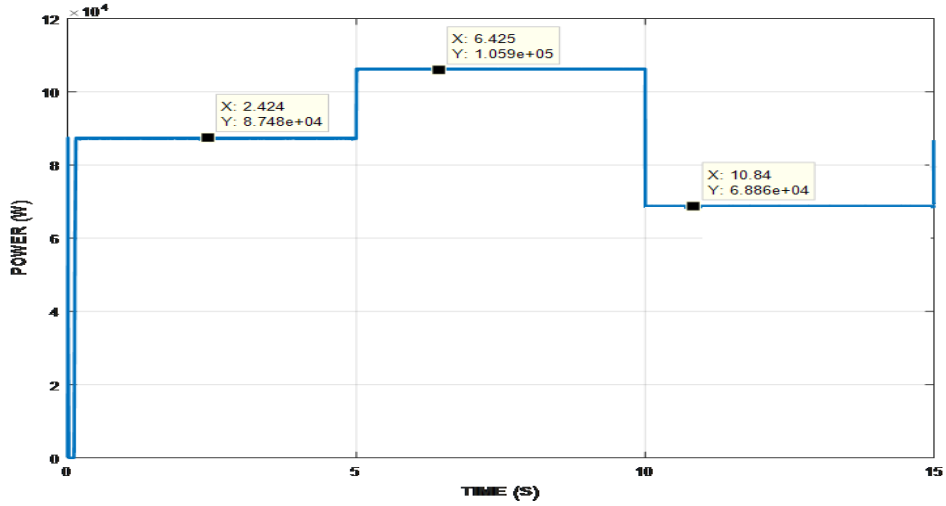

Fig (4.26). The Power Produced For The System During The Change Of The Rate Of Solar Radiation

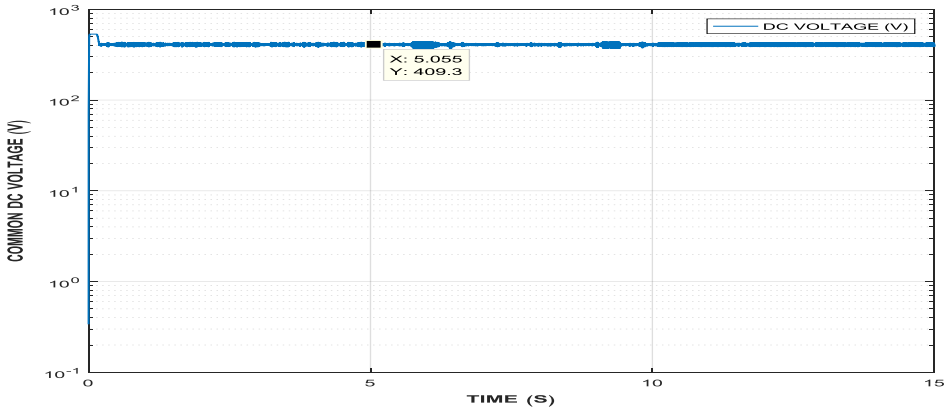

Fig (4.27). Common dc-Bus Voltage

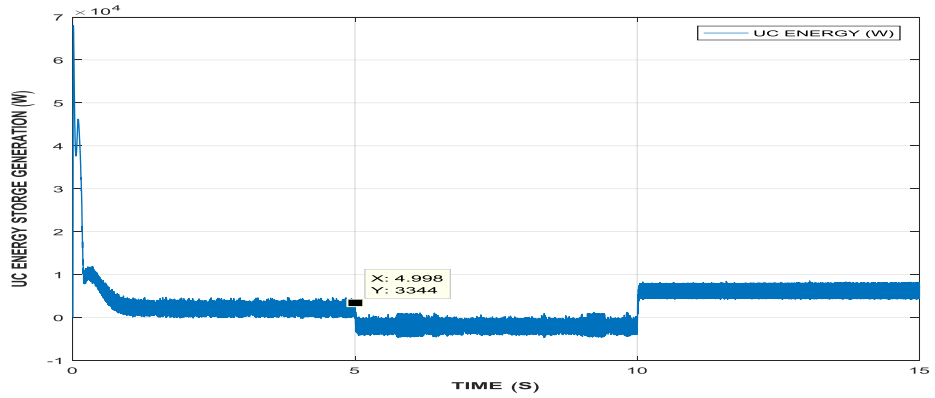

Fig (4.28). UC Energy Storage System Generation, Common DC-Bus Voltage

Figure (4.29), shows the alternating power produced by the system injected into the electrical loads during fluctuation of radiation rates.

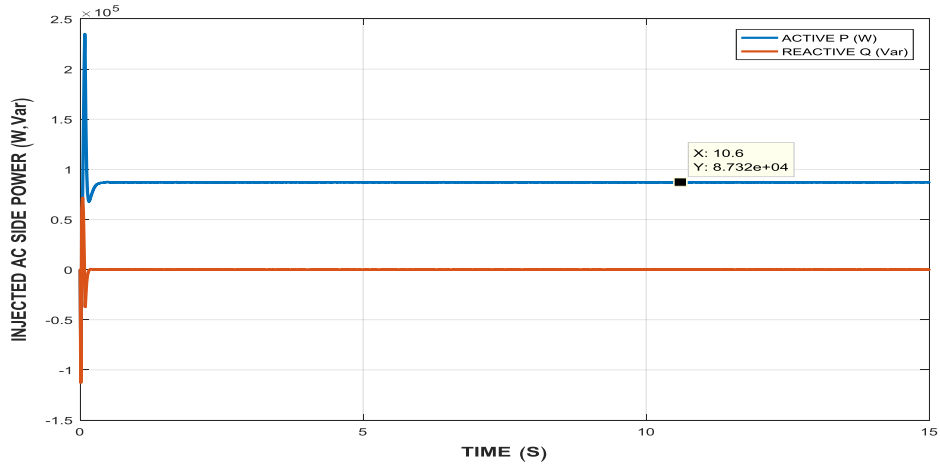

Fig (4.29). Active And Reactive Power At PCC

The previous figure shows that the alternating power that is injected into the network in PCC to be dispersed by the changes that occur in the side of the solar system in order to use the constant voltage transformer with the technique of tracking the maximum power point, which in turn maintains the value of the continuous voltage entering the AC voltage transformer during the disturbances that occur to the system, including. The change in the rates of solar radiation, which causes the system to produce a constant power as well as feeding the loads with a stable alternating power without any disturbances mentioned as shown in figures (4.30)(4.31).

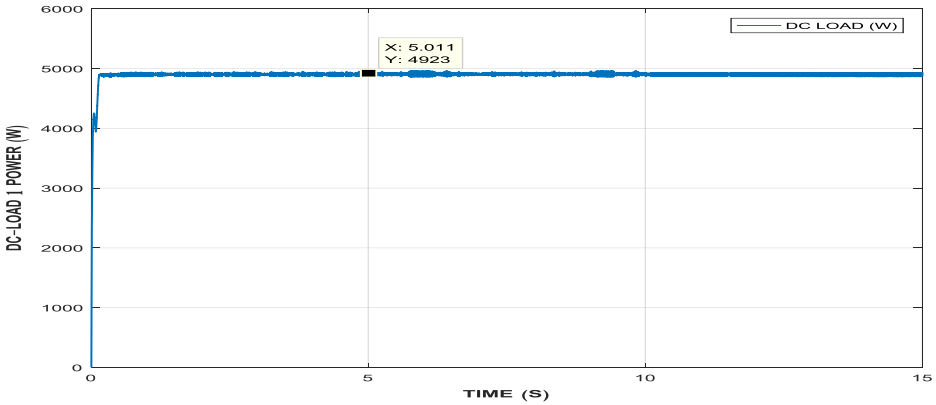

Fig (4.30). DC Load-1 Power

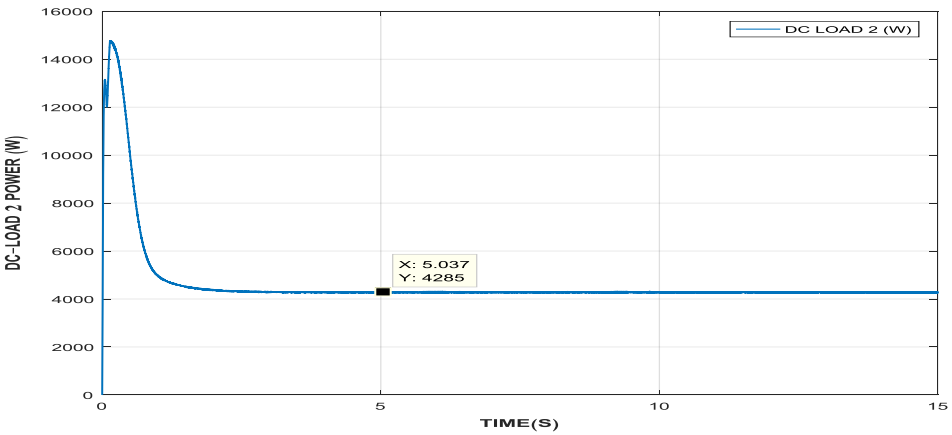

Fig (4.31). DC Load-2 Power

CHAPTER FIVE

CONCLUSION AND FUTURE WORK

5.1 CONCLUSION

- The modeling of hybrid microgrid for power system configuration is done in MATLAB/SIMULINK . The control mechanism of the system is used to maintain stable operation under various loads and resource conditions.
- MPPT algorithm is used to harness maximum power from DC sources and to coordinate the power exchange between DC and AC grid.
- The efficiency of the total system depends on the diminution of conversion losses.
- The hybrid grid can provide a reliable, high quality and more efficient power to consumer.
- The thesis shows how the renewable sources are integrated to the grid and are able to supply the power to the grid.
- The behavior of grid connected PV/Wind system under steady state operation has been investigated. At steady state speed of 15m/s and radiation 1000 W/m^2, the generation units operate stably and provide power for the loads.
- The obtained results showed that the system responds very well in this situations.

5.2 SCOPE OF FUTURE WORK

In this thesis ,there are still some improvements which need to be made and recommendations for future research:-

a. Study and design a smart PV system that contains grid tied system with storage battery ،where the smart system can decide when it should feed the energy in grid or storage in battery or connect the load home on the grid based on economic and technical consideration.

b. The control mechanism can be developed for a microgrid containing unbalanced and nonlinear loads.

c. Studying the behaviors of the whole system during line fault .

d. A laboratory setup should be made to verify the simulation results with the experimental tests. Further studies can still be done with hybrid system for research purposes .

REFERANCE

[1] Borowy BS, Salameh ZM, "Methodology for optimally sizing the combination of a battery bank and PV array in a wind/PV hybrid system, IEEE Transactions on Energy Conversion 1996; 11(2), 367-75 .

[2] Mohammed Gwani et.al, Urban Eco-Greenergy Hybrid Wind-Solar Photovoltaic Energy System & Its Applications, ISSN 2234-7593, International Journal of Precision Engineering & Manufacturing Vol.16, 2014 .

[3] Getachew Bekele, Design of a photovoltaic-wind hybrid power generation system for Ethiopian remote area, Energy Procedia 14 (2012) 1760 – 1765 .

[4] Jie Li et.al, Feasibility analysis of applying the wind-solar hybrid generation system in pastoral area, School of Information Engineering Inner Mongolia University of Science and Technology Baotou, China, 014010 {lijie_1963,c-y-4}@163.com (2012).

[5] D. Betha, M. Satish and S. K. Sahu, "Design and Control of Grid Connected PV/Wind Hybrid System Using 3 Level VSC," 2017 IEEE 7th International Advance Computing Conference (IACC), Hyderabad, 2017, pp. 466-471, doi: 10.1109/IACC.2017.0102..

[6] M.Tech. Scholar, Head " review on wind-solar hybrid power system " Department of Mechanical Engineering, G.H.Raisoni College of Engineering ،Nagpur, Maharashtra, India International Journal of Research In Science & Engineering March-April 2017.

[7] Arjun nair[1a], kartik murali[2b], anbuudayasankar.s.p[1c], c.v.arjunan[2a] " modelling and optimising the value of a hybrid solar -wind system " .

[1]Department of Mechanical Engineering, Amrita School of Engineering – Coimbatore, Amrita Vishwa Vidyapeetham University,Tamil Nadu, India. Pin – 641112

[2]Coimbatore Institute Engineering of technology, narasipuram road , Dist. Coimbatore, Narasipuram, tamil nadu 641109 , 2017.

[8] Soon ching chun " development of a hybrid solar wind turbine for sustainable energy storage " 2015.

[9] Damian b n nnadi, Charles I odeh, crescent omeje " use of hybrid solar-wind energy generation for remote area electrification in south-eastern Nigeria "Journal of Energy in Southern Africa 25(2): 61–69 DOI: http://dx.doi.org/10.17159/2413-3051/2014/v25i2a2670 .

[10] Jihane Kartite, Mohamed Cherkaoui " Study of the different structures of hybrid systems in renewable " Electrical Engineering Department, Mohammedia School of engineers , Rabat, MOROCCO, Corresponding author. Tel.:+212-658-67-3415. E-mail address: kartite.jihane@gmail.com 2018.

[11] Sumit Wagh , Pramod Walke " review on wind-solar hybrid power system " International Journal of Research In Science & Engineering e-ISSN: 2394-8299 p-ISSN: 2394-8280 Volume: 3 Issue:2 March-April 2017 .

[12] J. Aho et al., "A tutorial of wind turbine control for supporting grid frequency through active power control," 2012 American Control Conference (ACC), Montreal, QC, 2012, pp. 3120-3131, doi: 10.1109/ACC.2012.6315180. [13] John Wiley &Sons, Wind Energy Handbook, Cs-Books@Wiley.Co.Uk, Copyright 2001.

[14] Virgilio Centeno, Jaime De La Ree , Yilu Liu , Fred Wang , " The Modelling And Control Of A Wind Farm And Grid Interconnection In A Multi-Machine System", Doctor Of Philosophy In Electrical Engineering , August 26th, 2009 Blacksburg, Va From Pegs (2-7) .

[15] Tomas Petru, "Modelling Of Wind Turbines for Power System Studies", Department of Electric Power Engineering Chalmers University of Technology Gäoteborg, Sweden 2001.

[16] Centurion Energy. (2013, June 26). Types of Wind Turbines [Online]. Available.

[17] Directly at info@luvside.de or https://www.luvside.de/en/what-are-horizontal-axis-wind-turbines-hawt/ . This content was downloaded on 02/06/2020 at 14:50 .

[18] Michael A. Snyder , " Development Of Simplified Models Of Doubly-Fed Induction Generators (DFIG)" Master Of Science Thesis Department Of Energy And Environment Division Of Electric Power Engineering Chalmers University Of Technology G¨Oteborg, Sweden 2012 .

[19] Tarek abojila omer ahmed a thesis " Modeling and Simulation of Grid Connected AC Microgrid-Wind Turbine" university of zawia 2017.

[20] O. Anaya-Lara, "Wind Energy Generation Modelling and Control", John Wiley & Sons, New York, NY, USA, 2009.

[21] Michalke, G., & Hansen, A. D. (2010). "Modelling and control of variable speed wind turbines for power system studies". Wind Energy, 13(4), 307-322. https://doi.org/10.1002/we.341

[22] I. Pourfar, H. A. Shayanfar, H. M. Shanechi, and A. H. Naghshbandy, " Controlling PMSG-based wind generation by a locally available signal to damp power system inter-area oscillations" European Transaction on Electrical Power, 2012. First published: 15 May 2012 https://doi.org/10.1002/etep.1646 .

[23] Elprocus.com which contains various electronics concepts like circuits, projects ideas, etc. www.elprocus.com , This content was downloaded on 19/08/2020 at 23:13 .

[24] Babu, B. and S. Divya. "Comparative study of different types of generators used in wind turbine and reactive power compensation." (2017) .

[25] Wenping Cao, Ying Xie and Zheng Tan (November 21st 2012)." Wind Turbine Generator Technologies ", Advances in Wind Power, Rupp Carriveau, IntechOpen, DOI: 10.5772/51780. Available from: https://www.intechopen.com/books/advances-in-wind-power/wind-turbine-generator-technologies

[26] Ganesh kumar suman, suchit kumar sethi ‘‘modelling of double fed induction generator connected with wind turbine " Department of Electrical Engineering National Institute of Technology, Rourkela Rourkela-769008(ODISHA) May, 2014.

[27] Kun Han and Guo-zhu Chen, "A novel control strategy of wind turbine MPPT implementation for direct-drive PMSG wind generation imitation platform," 2009 IEEE 6th International Power Electronics and Motion Control Conference, Wuhan, 2009, pp. 2255-2259, doi: 10.1109/IPEMC.2009.5157778 .

[28] R Sitharthan, CK Sundarabalan, KR Devabalaji, T Yuvaraj and A Mohamed Imran " Automated power management strategy for wind power generation system using pitch angle controller " Date received: 6 July 2018; accepted: 27 December 2018.

[29] European Wind Energy Association. (2013, Nov. 4). How a Wind Turbine Works [Online]. Available: http://www.ewea.org/wind-energy- basics/how-a-wind-turbine-works/

[30] Fei Ding, Student Member, IEEE, and Kenneth A. Loparo, Fellow, IEEE, and Chengshan Wang ‘‘Modeling and Simulation of Grid-connected Hybrid AC/DC Microgrid " 2012 IEEE.

[31] Energy Research Unit (n.d.). (2013, Nov. 4). "Energy Research Unit Meteorological Data [Online]. Available" : http://www.elm.eru.rl.ac.uk/ins4.html , This content was downloaded on 12/08/2020 at 17:15 .

[32] Mwaniki, Julius, et al. "A Condensed Introduction to the Doubly Fed Induction Generator Wind Energy Conversion Systems." Journal of Engineering, vol. 2017, 2017. Gale Academic OneFile, . Accessed 25 Dec. 2020..

[33] D.Ali A. Mehna and Ibrahim E. Abdualkafi " Dynamic Modeling and Simulation of Grid-Connected PV-Wind Turbine Microgrid System using MATLAB/SIMULINK " .

[34] Camille Hamon , " Doubly-Fed Induction Generator Modeling And Control In Dig Silent Power Factory", Master’s Thesis At Kth School Of Electrical Engineering , Xr-Ee-Es 2010:004.

[35] Lipsa priyadarshanee " modelling and control of hybrid ac/dc micro grid ‘‘.Department of Electrical Engineering National Institute of Technology Rourkela-769008 (2010-2012) .

[36] Kumar, Sandeep (2014) "Modeling and simulation of hybrid wind/photovoltaic stand-alone generation system ‘‘.

[37] Nayak, P.K., Mahesh, S., Snaith, H.J. et al. "Photovoltaic solar cell technologies: analysing the state of the art". Nat Rev Mater 4, 269–285 (2019). https://doi.org/10.1038/s41578-019-0097-0.

[38] Saeed Atallah "What are solar cells". (https://www.arageek.com/l/) , 2020 . This content was downloaded on 24/08/2020 at 09:00 .

[39] Chapter 2 "mathematical modelling of photovoltaic system" , This content was downloaded on 17/09/2020 at 12:05 .
https://webcache.googleusercontent.com/search?q=cache:cLHS_sEMPHUJ:https://shodhganga.inflibnet.ac.in/bitstream/10603/173729/12/12_chapter%25202.pdf+&cd=15&hl=ar&ct=clnk&gl=ly&client=firefox-b-d

[40] engineering.com " Challenges of Making Solar Energy Economical " 2019 https://www.engineering.com/DesignerEdge/DesignerEdgeArticles/ArticleID/19841/Challenges-of-Making-Solar-Energy-Economical.aspx , This content was downloaded on 20/09/2020 at 11:34

[41] Abdelaziz El Ghzizal[1], Souad Sebti[1], and Aziz Derouich[1] (2018) "Modeling of Photovoltaic System with Modified Incremental Conductance Algorithm for Fast Changes of Irradiance" [1]Laboratory of Production Engineering, Energy and Sustainable Development, Higher School of Technology, SMBA University, Fez, Morocco.

[42] Adel A. Elbaset M.S. Hassan " Design and Power Quality Improvement of Photovoltaic Power System 2017.

[43] Othman, A.M., Gabbar, H.A. and Honarmand, N. (2015) " Performance Analysis of Grid Connected and Islanded Modes of AC/DC Microgrid for Residential " Home Cluster. Intelligent Control and Automation, 6, 249-270 . http://dx.doi.org/10.4236/ica.2015.64024 .

[44] A. Khalil, K. A. Alfaitori and A. Asheibi, "Modeling and control of PV/Wind Microgrid," 2016 7th International Renewable Energy Congress (IREC), Hammamet, 2016, pp. 1-6, doi: 10.1109/IREC.2016.7478916" .

[45] M. S. Hossain, N. K. Roy and M. O. Ali, "Modeling of solar photovoltaic system using MATLAB/Simulink," 2016 19th International Conference on Computer and Information Technology (ICCIT), Dhaka, 2016, pp. 128-133, doi: 10.1109/ICCITECHN.2016.7860182.

[46] Amit Kumar Sharma, Ravinder Singh Chauhan, Gaurav Rajoria(2016) " Mathematical Modeling and Simulation of Photovoltic Array " , Amit Kumar Sharma. et. al. Int. Journal of Engineering Research and Applications www.ijera.com ISSN: 2248-9622, Vol. 6, Issue 3, (Part - 6) March 2016, pp.74-76.

[47] Furkan Dinçer, Mehmet Emin Meral(2010) " Critical Factors that Affecting Efficiency of Solar Cells" University of Yuzuncu Yil, Department of Electrical and Electronics Engineering, Van, Turkey doi: 10.4236/sgre.2010.11007.

[48] Pushprajsinh thakor, aakashkumar chavada, bhargviben patel. " Comparative analysis of different mppt techniques for solar pv system " International Research Journal of Engineering and Technology (IRJET), e-ISSN: 2395 -0056 , p-ISSN: 2395-0072 , May-2016.

[49] Rasika Chitnis, Naushin Khan " Outline of the various MPPT methods used for photovoltaic power control " International Journal of Recent Trends in Engineering & Research (IJRTER) Volume 02, Issue 06; June - 2016 [ISSN: 2455-1457] .

[50] CH Hussaian Basha and C Rani " Different Conventional and Soft Computing MPPT Techniques for Solar PV Systems with High Step-Up Boost Converters: A Comprehensive Analysis " School of Electrical Engineering, VIT University, Vellore 632014, India ؛(sbasha238@gmail.com) Correspondence: crani@vit.ac.in Received: 4 December 2019; Accepted: 10 January 2020; Published: 12 January 2020.

[51] Hegazy Rezk, Ali M. Estimably " A comprehensive comparison of different MPPT techniques for photovoltaic systems " E-mail addresses: hegazy.hussien@mu.edu.eg (H. Rezk),

eltamaly@ksu.edu.sa (A.M. Eltamaly). http://dx.doi.org/10.1016/j.solener.2014.11.010 0038-092X/© 2014 Elsevier Ltd. All rights reserved. 2014.

[52] Ramdan B. A. Koad, Ahmed. F. Zobaa " Comparative study of five maximum power point tracking techniques for photovoltaic systems " January 2014 International Journal on Energy Conversion (IRECON) 2(1):17 DOI: 10.15866/irecon.v2i1.1437.

[53] Ibrahim Emhemmed Abdualkafi " modelling and simulation of grid–connected photovoltaic system " 2015.

[54] B. Chitti Babu, T. Cermak, S. Gurjar, Z. M. Leonowicz and L. Piegari, "Analysis of mathematical modeling of PV module with MPPT algorithm," 2015 IEEE 15th International Conference on Environment and Electrical Engineering (EEEIC), Rome, 2015, pp. 1625-1630, doi: 10.1109/EEEIC.2015.7165415.

[55] Sengar, S.. "Maximum Power Point Tracking Algorithms for Photovoltaic System : A Review." (2014) International Review of Applied Engineering Research.ISSN 2248-9967 Volume 4, Number 2 (2014), pp. 147-154© Research India Publications http://www.ripublication.com/iraer.htm .

[56] Mohannad Jabbar Mnati, Victor Gino Morais Araujo, Jameel Kadhim Abed Alex Van den Bossche " Review Different Types of MPPT Techniques for Photovoltaic Systems " June 2018 Conference: International Conference on Sustainable Energy and Environment Sensing (SEES 2018)At: Venue: Fitzwilliam College, University of Cambridge, Cambridge city, United Kingdom.

[57] Athira B . Greeshma V. Jeena Johnson " Analysis of Different MPPT Techniques " International Journal of Advanced Research in Electrical,Electronics and Instrumentation Engineering(An ISO 3297: 2007 Certified Organization Vol. 5, Issue 3, March 2016.

[58] Awonke Nkophe " Application of MATLAB/SIMULINK in Solar PV Systems " ©Springer International Publishing Switzerland 2015S. Sumathi et al ،.Solar PV and Wind Energy Conversion Systems,Green Energy and Technology, DOI 10.1007/978-3-319-14941-7_2.

[59] Nur Atharah Kamarzaman, Chee Wei Tan " A comprehensive review of maximum power point tracking algorithms for photovoltaic systems " 2014 E-mail addresses: cheewei@fke.utm.my,dr. c.w.tan@gmail.com (C.W. Tan) . http://dx.doi.org/10.1016/j.rser.2014.05.045 1364-0321/&2014 Elsevier Ltd. All rights reserved.n .

[60] A. Kchaou, A. Naamane, Y. Koubaa and N. K. M'Sirdi, "Comparative study of different MPPT techniques for a stand-alone PV system," 2016 17th International Conference on Sciences and Techniques of Automatic Control and Computer Engineering (STA), Sousse, 2016, pp. 629-634, doi: 10.1109/STA.2016.7952092.

[61] El-Shahat A, Sumaiya S. DC-Microgrid System Design, Control, and Analysis. https://doi.org/10.3390/electronics8020124 Electronics. 2019; 8(2):124.

[62] B. Gundersen, "An investigation on grid connectable single phase photovoltaic inverters," Master of Science in Energy and Environment January 2010.

[63] Anwarul m haque. swati sharma, devendra nagal " simulation of photovoltaic system connected with full bridge inverter using matlab / simulink " Volume: 05 Issue: 01 | Jan-2016, Available @ http://www.ijret.org .

[64] Ravi Kansagara " Introduction to Different Types of Inverters " Dec 18, 2018 .

[65] Nabil Karami ،Nazih Moubayed, Rachid Outbib ‘‘General review and classification of different MPPT Techniques " Renewable and Sustainable Energy Reviews, 2017, vol. 68, issue P1, 1-18.

[66] S. Sumathi et al " Solar PV and Wind Energy Conversion Systems Green Energy and Technology " Springer International Publishing Switzerland 2015 Print ISBN: 978-3-319-14940-0 Electronic ISBN: 978-3-319-14941-7.

[67] Soeren Baekhoej Kjaer, John K. Pedersen and Frede Blaabjerg, “A Review of Single Phase Grid-Connected Inverters for Photovoltaic Modules,” IEEE Transactions of Industry Applications, Vol. 41, No. 5, pp. 1292-1306, September/October 2005 .

[68] Svein Erik Evju. Fundamentals of Grid Connected Photovoltaic Power Electronic Converter Design. Specialization project, Department of Electric Engineering, Norwegian University of Science and Technology, December 2006.

[69] System sizing: http://www.iea- shc.org/outputs/ photovoltaics_ in_ buildings. Data acessed 12-11-2020, Time, 10:23PM.